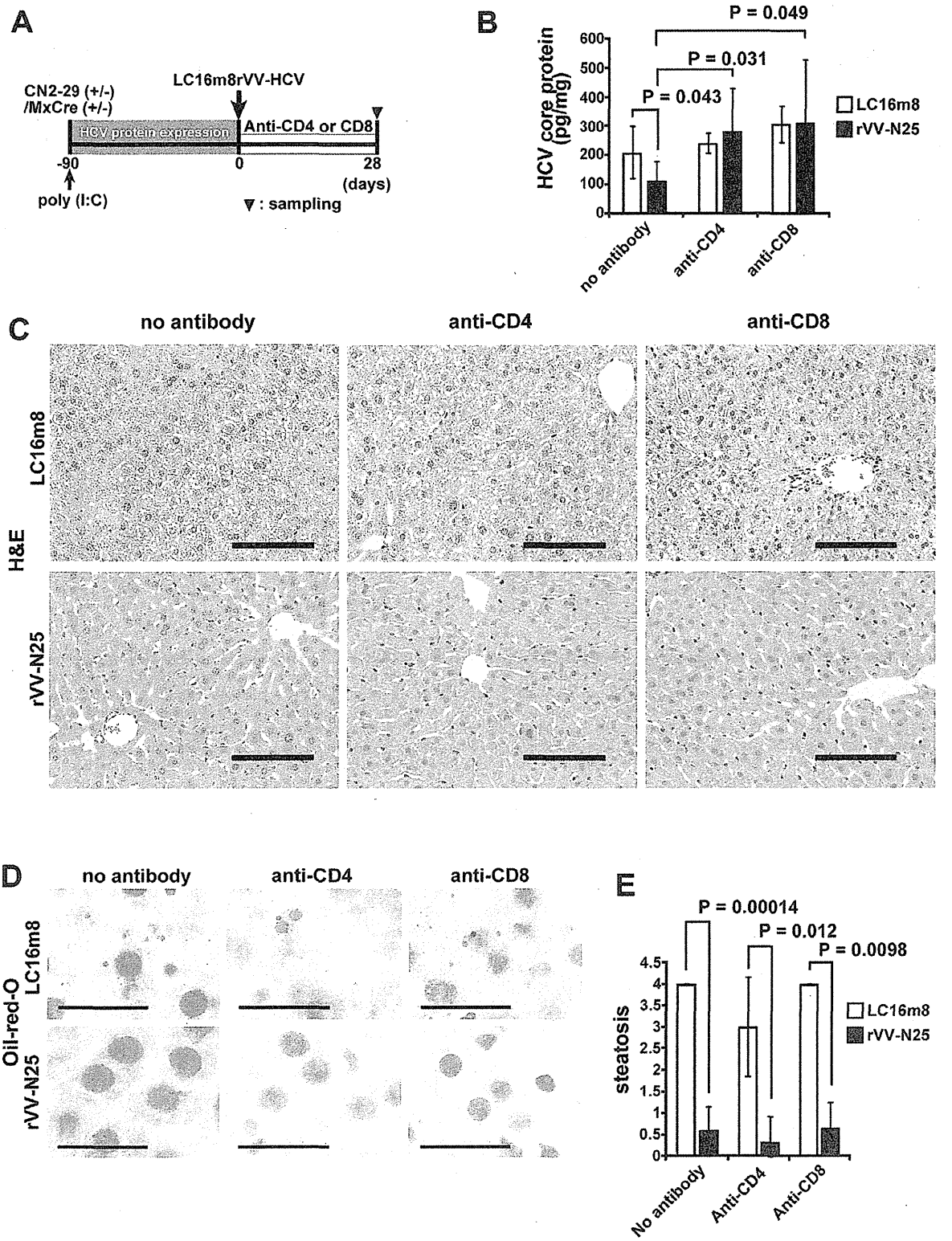

Figure 4. Role of CD4 and CD8 T cells in rVV-N25-treated mice. (**A**) Schematic diagram depicts depletion of CD4 and CD8 T cells via treatment with monoclonal antibodies. (**B**) Comparison of HCV core protein expression in control, CD4-depleted, and CD8-depleted mice 28 days after immunization with LC16m8 or rVV-N25. (**C, D**) Histological analysis of liver samples from CD4-depleted or CD8-depleted CN2-29$^{(+/-)}$/MxCre$^{(+/-)}$ mice

28 days after immunization with LC16m8 or rVV-N25. The scale bars indicate 100 μm (**C**) and 50 μm (**D**). (**E**) Histological evaluation of steatosis in liver samples from CD4-depleted or CD8-depleted CN2-29$^{(+/-)}$/MxCre$^{(+/-)}$ mice 28 days after immunization with LC16m8 or rVV-N25. Significant relationships are indicated by a P-value.
doi:10.1371/journal.pone.0051656.g004

a HCV nonstructural protein. Thus, we focused on the role of the NS2 region as the target for CD8 T cells and generated EL-4 cell lines that expressed the NS2 antigen or the CN2 antigen.

Isolated splenocytes from immunized mice were co-cultured with EL-4CN2 or EL-4NS2 cell lines for 2 weeks and analyzed.

Cytolytic cell activation can be measured using CD107a, a marker of degranulation [15]. The ratio of CD8$^+$CD107a$^+$ cells to all CD8 T cells significantly increased in rVV-N25-treated splenocytes after co-culture with EL-4CN2 or EL-4NS2 ($P<0.05$), whereas splenocytes that had been treated with any other rVV were not detected (Figure 5A, B and C). These results indicated that rVV-N25 treatment increased the frequency of HCV NS2-specific activated CD8 T cells. Consistent with these results, the ratio of CD8$^+$IFN-γ$^+$ cells to all CD8 T cells for rVV-N25-treated mice was also significantly higher than that for mice treated with any other rVV ($P<0.05$). Taken together, these findings indicated that rVV-N25 induced an effective CD8 T-cell immune response and that NS2 is an important epitope for CD8 T cells.

rVV-N25 Immunization Suppressed Inflammatory Cytokines Production

To determine whether rVV-N25 treatment affected inflammatory cytokine production, we measured serum levels of inflammatory cytokines after rVV immunization. The serum levels of these inflammatory cytokines increased in the CN2-29$^{(+/-)}$/MxCre$^{(+/-)}$ mice (Figure 6A, Figure S5). Immunization with rVV-N25 affected serum levels of inflammatory cytokines in CN2-29$^{(+/-)}$/MxCre$^{(+/-)}$ mice and caused a return to the cytokine levels observed in wild-type untreated mice (Figure 6A). In wild-type mice, the cytokine levels remained unchanged after immunization (Figure 6A). These results indicated that inflammatory cytokines were responsible for liver pathogenesis in the transgenic mice.

To test the hypothesis that inflammatory cytokines were responsible for liver pathogenesis in CN2-29$^{(+/-)}$/MxCre$^{(+/-)}$ mice, we administered transgenic mouse serum intravenously into nontransgenic mice. We observed the development of chronic hepatitis in the nontransgenic mice within 7 days after the serum transfer (Figures 6B and C). This finding was consistent with the

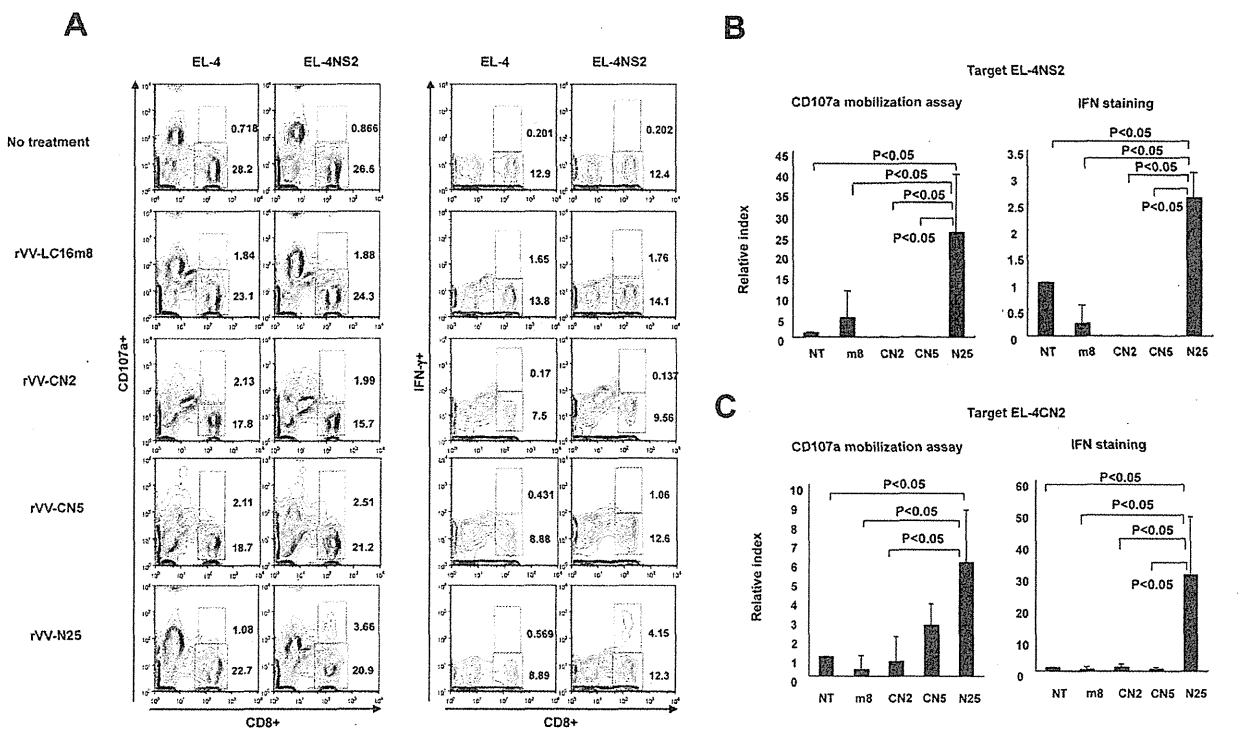

Figure 5. Immunization with rVV-N25 induced CD8 T-cell degranulation, a marker for cytotoxicity, and IFN-γ production. (**A**) The numbers represent the percentage of CD107a positive cells and negative cells (left two columns) and IFN-γ-positive cells and negative cells (right two columns). (**B, C**) The ratio of CD8$^+$IFN-γ$^+$ cells to all CD8 T cells for rVV-N25-treated mice was significantly higher than that for mice treated with any other rVV. Splenocytes (4 × 10^6 per well) were cultured with EL-4CN2 or EL-4NS2 cell lines in RPMI 1640 complete medium including 3% T-STIM^{TM} with ConA for 2 weeks. Harvested cells were incubated for 4 h with EL-4, EL-4CN2, or EL-4NS2 in combination with PE-labeled anti-CD107a mAb and monensin in RPMI 1640 complete medium with 50 IU/mL IL-2, according to the manufacturer's instruction. After incubation, cell suspensions were washed with PBS, and the cells were further stained with APC-labeled anti-IFN-γ mAb and Pacific blue-labeled anti-CD8 mAb. Harvested cells were stained with anti-CD107a-PE, anti-IFN-γ-APC, or anti-CD8-Pacific blue. Results that are representative of three independent experiments are shown. Significant relationships are indicated by P-value.
doi:10.1371/journal.pone.0051656.g005

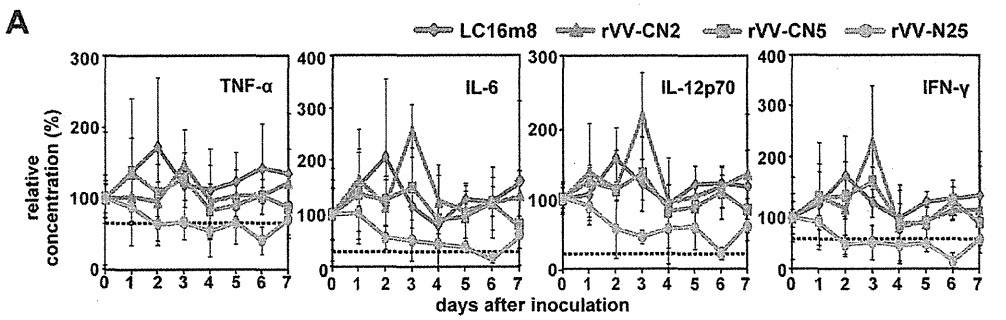
A
LC16m8
rVV-CN2
rVV-CN5
rVV-N25
TNF-α
IL-6
IL-12p70
IFN-γ
relative concentration (%)
days after inoculation

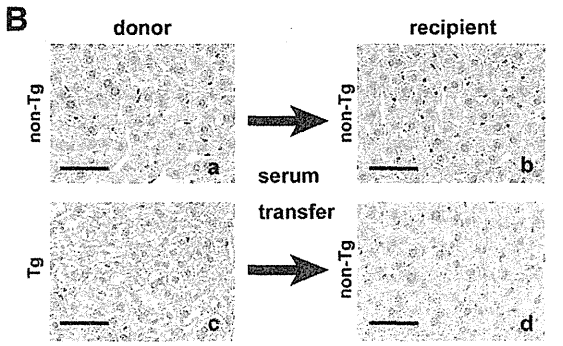
B
donor
recipient
non-Tg
Tg
serum transfer
a
b
c
d

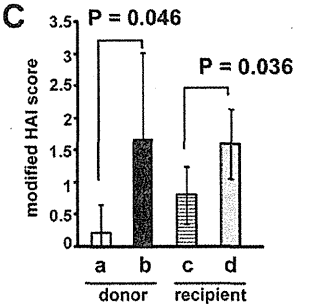
C
P = 0.046
P = 0.036
modified HAI score
a b c d
donor
recipient

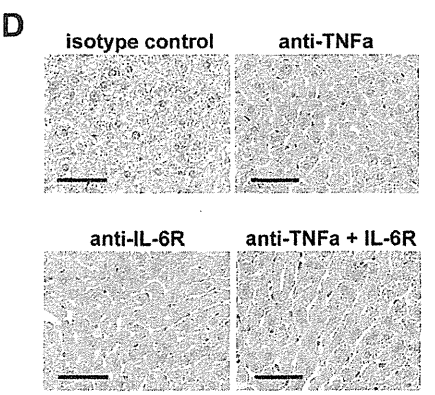
D
isotype control
anti-TNFa
anti-IL-6R
anti-TNFa + IL-6R

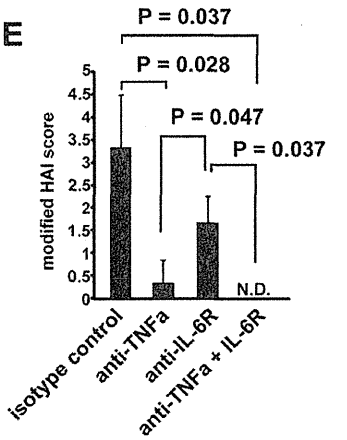
E
P = 0.037
P = 0.028
P = 0.047
P = 0.037
N.D.
modified HAI score
isotype control
anti-TNFa
anti-IL-6R
anti-TNFa + IL-6R

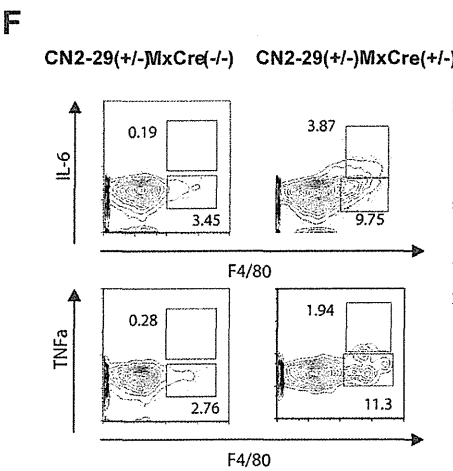
F
CN2-29(+/-)MxCre(-/-)
CN2-29(+/-)MxCre(+/-)
IL-6
TNFa
F4/80
0.19
3.45
3.87
9.75
0.28
2.76
1.94
11.3

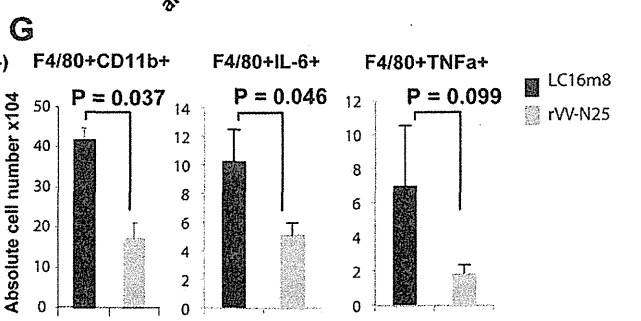
G
F4/80+CD11b+
F4/80+IL-6+
F4/80+TNFa+
P = 0.037
P = 0.046
P = 0.099
Absolute cell number x10⁴
LC16m8
rVV-N25

Figure 6. Immunization with rVV-N25 suppresses serum inflammatory cytokine levels. (**A**) Daily cytokine levels in the serum of CN2-29$^{(+/-)}$/MxCre$^{(+/-)}$ mice during the week following immunization with LC16m8, rVV-CN2, rVV-N25, or rVV-CN5. Values represent means ± SD (n = 3) and reflect the concentrations relative to those measured on day 0. The broken lines indicate the baseline data from wild-type mice. In all cases, n = 6 mice per group. (**B**) Liver sections from CN2-29$^{(+/-)}$/MxCre$^{(+/-)}$ and CN2-29$^{(+/-)}$/MxCre$^{(-/-)}$ mice. (**C**) Histology activity index (HAI) scores of liver samples taken from CN2-29$^{(+/-)}$/MxCre$^{(+/-)}$, or CN2-29$^{(+/-)}$/MxCre$^{(-/-)}$ mice. (**D**) Liver sections from CN2-29$^{(+/-)}$/MxCre$^{(+/-)}$ mice in which TNF-α was neutralized and the IL-6 receptor was blocked. The scale bars indicate 50 μm. (**E**) HAI scores of liver samples taken from CN2-29$^{(+/-)}$/MxCre$^{(+/-)}$ in which TNF-α was neutralized and the IL-6 receptor was blocked. Tg and non-Tg indicate CN2-29$^{(+/-)}$/MxCre$^{(+/-)}$ and CN2-29$^{(+/-)}$/MxCre$^{(-/-)}$, respectively. (F) Macrophages were the main producers of TNF-α and IL-6 in CN2-29$^{(+/-)}$/MxCre$^{(+/-)}$ mice following poly(I:C) injection. (G) Immunization with rVV-N25 reduced the number of macrophages in liver samples from CN2-29$^{(+/-)}$/MxCre$^{(+/-)}$ mice and suppressed TNF-α and IL-6 production from macrophages (Figure 6G). Significant relationships are indicated by a P-value.
doi:10.1371/journal.pone.0051656.g006

hypothesis that inflammatory mediators played a key role in inducing hepatitis. Furthermore, to investigate whether TNF-α and IL-6 played particularly critical roles in the pathogenesis of chronic hepatitis in the transgenic mice, we neutralized TNF-α and blocked the IL-6 receptor in the livers of these mice. As expected, chronic hepatitis did not develop in these mice. (Figure 6D and E).

Next, to determine which cell population(s) produced TNF-α, IL-6, or both during continuous HCV expression in CN2-29$^{(+/-)}$/MxCre$^{(+/-)}$ mice, we isolated intrahepatic lymphocytes (IHLs) and labeled the macrophages (the F4/80^{+} cells) with anti-TNF-α and anti-IL-6 antibodies using an intracellular cytokine detection method. Macrophages in CN2-29$^{(+/-)}$/MxCre$^{(-/-)}$ mice produced small amounts of TNF-α and IL-6, while those in CN2-29$^{(+/-)}$/MxCre$^{(+/-)}$ mice produced much larger amounts of these cytokines (Figure 6F).

Finally, we evaluated whether rVV-N25 treatment affected the number of macrophages, cytokine production by macrophages, or both; specifically, we isolated IHLs from CN2-29$^{(+/-)}$/MxCre$^{(+/-)}$ mice 7 days after immunization with rVV-N25 or with LC16m8. The percentage of macrophages (CD11b^{+}F4/80^{+}) among IHLs and IL-6 production from these macrophages were significantly lower in rVV-N25-treated mice than in control mice (Figure 6G). Though the percentage of TNF-α-producing macrophages was not significantly different in rVV-N25-treated and control mice ($P = 0.099$), rVV-N25 treatment appeared to suppress these macrophages. These results demonstrated that rVV-N25 had a suppressive effect on activated macrophages, and they indicated that this suppression ameliorated the histological indicators of chronic hepatitis.

Discussion

Various HCV transgenic mouse models have been developed and used to examine immune response to HCV expression and the effects of pathogenic HCV protein on hepatocytes [4,16,17]. However, these transgenic mice develop tolerance to the HCV protein; therefore, examining immune response to HCV protein has been difficult.

To overcome the problem of immune tolerance in mouse models of HCV expression, we developed an HCV model in mice that relies on conditional expression of the core, E1, E2, and NS2 proteins and the Cre/loxP switching system [5,6]; we showed that the injection of an Ad-Cre vector enhanced the frequency of HCV-specific activated CD8 T cells in the liver of these mice and caused liver injury. However, the Ad-Cre adenovirus vector alone causes acute hepatitis in wild-type mice. Nevertheless, the transgenic model was useful for evaluating interactions between the host immune system and viral protein (serum ALT level over 2,000 IU/L) [5]; HCV core protein levels were reduced and expression of this protein was transient (about 2 weeks). Therefore, this Ad-Cre-dependent model cannot be used to effectively investigate immune responses to chronic HCV hepatitis.

Here, we used poly (I:C)-induced expression of Cre recombinase to generate HCV transgenic mice in order to study the effect of HCV protein and confirmed that these mice developed chronic active hepatitis–including steatosis, lipid deposition, and hepatocellular carcinoma. These pathological findings in the transgenic mice were very similar to those in humans with chronic hepatitis C; therefore, this mouse model of HCV may be useful for analyzing the immune response to chronic hepatitis. However, experimental results obtained with this mouse model may not directly translate to clinical findings from patients with HCV infection because the expression of HCV proteins was not liver specific in these mice. Furthermore, poly(I:C) injection can activate innate immune responses and, consequently, might induce temporary liver injury [18]. Additionally, poly(I:C) injection has an adjuvant effect; specifically, it stimulates TLR3 signaling [19].

To evaluate whether poly(I:C) injection caused hepatitis in CN2-29$^{(+/-)}$/MxCre$^{(-/-)}$ mice, we examined serum ALT levels and liver histology following poly(I:C) injection. We found that, following poly(I:C) injection, serum ALT levels in CN2-29$^{(+/-)}$/MxCre$^{(-/-)}$ mice increased, reached a peak one day after injection, declined from day 1 to day 6, and were not elevated thereafter; this time-course indicated that poly(I:C) injection alone did not induced continuous liver injury (figure S6). Based on these findings, we believe that the effects of poly(I:C) injection in these mice did not confound our analysis of chronic hepatitis.

Immunization with rVV-N25 suppressed HCV protein levels in the liver, and this suppression was associated with ameliorated pathological chronic hepatitis findings (see Figure 3). Importantly, rVV-N25 treatment did not cause liver injury based on the serum ALT levels; therefore, this treatment was unlikely to have cytopathic effects on infected hepatocytes. These findings provided strong evidence that rVV-N25 treatment effectively halted the progression of chronic hepatitis. Immunization with plasmid DNA or with recombinant vaccinia virus can effectively induce cellular and humoral immune responses and exert a protective effect against challenge with HCV infection [20,21]. However, findings from these previous studies revealed HCV immunization of both uninfected, naïve animals and immune-tolerant animals induced a HCV-specific immune response. In the model describe here; the animals were immune competent for HCV; therefore, our findings provided further important evidence that rVV-N25 was effective in the treatment of chronic hepatitis.

In addition, we demonstrated that rVV-N25 treatment in the absence of CD4 and CD8 T cells had no effect on HCV clearance. This important observation indicated that rVV-N25-induced HCV clearance was mediated by CD4 and CD8 T cells. Many studies have shown that spontaneous viral clearance during acute HCV infection is characterized by a vigorous, broadly reactive CD4 and CD8 T-cell response. [8,22] HCV clearance and hepatocellular cytotoxicity are both mediated by CD8 antigen-specific (cytotoxic T lymphocyte) CTLs [23]. Consistent with these observations, rVV-N25 treatment effectively induced the accumulation of NS2-specific CD8 T cells, which express high levels of

CD107a and IFN-γin the spleen. Notably, even with rVV-N25 immunization, the frequency of activated CD8 T cells was very low, and a minimum of 2-weeks incubation was required to distinguish the difference between rVV treatments. Even if a small population of specific CD8+ T cells played a relevant role in the reduction of core protein, it is difficult to assert that the only NS2-specific CD8+ T cells were important to this reduction. However, based on the results presented in Figure 4B, we are able to conclude that at least CD8+ and/or CD4+ T cells were important to the reduction in HCV core protein. Therefore, to elucidate the mechanism of HCV protein clearance, further investigation of not only the other T cell epitopes but also other immunocompetent cells is required.

Interestingly, rVV-N25 treatment–but not the rVV-CN2 or rVV-CN5 treatment–efficiently induced a HCV-specific activated CD8 T cells response; this difference in efficacy could have one or more possible causes. The HCV structural proteins (core, E1, and E2 proteins) in the rVV-CN construct may cause the difference; Saito et al. reported that injection with plasmid constructs encoding the core protein induced a specific CTL response in BALB/c mice [24]. Reportedly, CTL activity against core or envelope protein is completely absent from transgenic mice immunized with a plasmid encoding the HCV structural proteins, but core-specific CTL activity is present in transgenic mice that were immunized with a plasmid encoding the HCV core [21]. In contrast, when recombinant vaccinia virus expressing different regions of the HCV polyprotein were injected into BALB/c mice, only the HCV core protein markedly suppressed vaccinia-specific CTL responses [25]. Thus, the HCV core protein may have an immunomodulatory function [26]. Based on these reports and our results, we hypothesize that the causes underlying the effectiveness of rVV-N25 treatment were as follows: 1) this rVV construct included the core and envelope proteins and 2) the core protein had an immune-suppressive effect on CTL induction. Therefore, we suggest that exclusion of the core and envelope antigen as immunogen is one important factor in HCV vaccine design.

Interestingly, immunization with rVV-N25 rapidly suppressed the inflammatory response; however, immunization with either of the other rVVs did not (see Figure 6A). This result indicated that rVV-N25 may modulate inflammation via innate immunity, as well as via acquired immunity. Reportedly, Toll-like receptor (TLR)-dependent recognition pathways play a role in the recognition of poxviruses [27]. TLR2 and TLR9 have also been implicated in the recognition of the vaccinia virus [28,29]. These findings indicate that TLR on dendritic cells may modulate the immunosuppressive effect of rVV-N25 in our model of HCV infection; however, further examination of this hypothesis is required. The finding that pathological symptoms in the HCV transgenic mice were completely blocked by intravenous injection of TNF-α and IL-6 neutralizing antibodies indicated that the progression of chronic hepatitis depended on inflammatory cytokines in serum, rather than the HCV protein levels in hepatocytes. Lymphocytes, macrophages, hepatocytes, and adipocytes each produce TNF-α and IL-6 [30,31], and HCV-infected patients have elevated levels of TNF-α and IL-6 [32,33]. Both cytokines also contribute to the maintenance of hepatosteatosis in mice fed a high-fat diet [34], and production of TNF-α and IL-6 is elevated in obese mice due to the low grade inflammatory response that is caused by lipid accumulation [35]. These findings indicate that both cytokines are responsible for HCV-triggered hepatosteatosis, and anti-cytokine neutralization is a potential treatment for chronic hepatitis if antiviral therapy is not successful.

The reduction of macrophages in number might be due to the induction of apoptosis by vaccinia virus *in vitro* infection as previous reported [36]. To understand the mechanisms responsible for the reduction of the number of macrophage, we performed another experiment to confirm whether the macrophages were infected with vaccinia virus inoculation. However, based on PCR analyses; vaccinia virus DNA was not present in liver tissue that contained macrophages (Figure S7). Furthermore, apoptosis of macrophages was not detected in liver samples (Data not shown). Based on these results, it is unlikely that the reduction in the number of macrophages was due to apoptosis induced by vaccinia virus infection. Although rVV-N25 reduced the number of macrophage, precise mechanism is still unknown. Further examination to elucidate the mechanism is required.

In conclusion, our findings demonstrated that rVV-N25 is a promising candidate for an HCV vaccine therapy. Additionally, the findings of this study indicate that rVV-N25 immunization can be used for prevention of HCV infection and as an antiviral therapy against ongoing HCV infection.

Materials and Methods

Ethics Statement

All animal care and experimental procedures were performed according to the guidelines established by the Tokyo Metropolitan Institute of Medical Science Subcommittee on Laboratory Animal Care; these guidelines conform to the Fundamental Guidelines for Proper Conduct of Animal Experiment and Related Activities in Academic Research Institutions under the jurisdiction of the Ministry of Education, Culture, Sports, Science and Technology, Japan, 2006. All protocols were approved by the Committee on the Ethics of Animal Experiments of the Tokyo Metropolitan Institute of Medical Science (Permit Number: 11–078). All efforts were made to minimize the suffering of the animals.

Animals

R6CN2 HCV cDNA (nt 294–3435) [37] and full genomic HCV cDNA (nt 1–9611) [38,39] were cloned from a blood sample taken from a patient (#R6) with chronic active hepatitis (Text S1). The infectious titer of this blood sample has been previously reported [40]. R6CN2HCV and R6CN5HCV transgenic mice were bred with Mx1-Cre transgenic mice (purchased from Jackson Laboratory) to produce R6CN2HCV-MxCre and R6CN5HCV-MxCre transgenic mice, which were designated CN2-29$^{(+/-)}$/MxCre$^{(+/-)}$ and RzCN5-15$^{(+/-)}$/MxCre$^{(+/-)}$ mice, respectively. Cre expression in the livers of these mice was induced by intraperitoneal injection of polyinosinic acid–polycytidylic acid [poly(I:C)] (GE Healthcare UK Ltd., Buckinghamshire, England); 300 μL of a poly(I:C) solution (1 mg/mL in phosphate-buffered saline [PBS]) was injected three times at 48-h intervals. All animal care and experimental procedures were performed according to the guidelines established by the Tokyo Metropolitan Institute of Medical Science Subcommittee on Laboratory Animal Care.

Histology and Immunohistochemical Staining

Tissue samples were fixed in 4% paraformaldehyde in PBS, embedded in paraffin, sectioned (4-μm thickness), and stained with hematoxylin and eosin (H&E). Staining with periodic acid–Schiff stain, Azan stain, silver, or Oil-red-O was also performed to visualize glycogen degeneration, fibrillization, reticular fiber degeneration, or lipid degeneration, respectively.

For immunohistochemical staining, unfixed frozen liver sections were fixed in 4% paraformaldehyde for 10 min and then incubated with blocking buffer (1% bovine serum albumin in PBS) for 30 min at room temperature. Subsequently, the sections were incubated with biotinylated mouse anti-HCV core mono-

clonal antibody (5E3) for 2 h at room temperature. After being washed with PBS, the sections were incubated with streptavidin–Alexa Fluor 488 (Invitrogen). The nuclei were stained with 4',6-diamidino-2-phenylindole (DAPI). Fluorescence was observed using a confocal laser microscope (Laser scanning microscope 510, Carl Zeiss).

Generation of rVVs

The pBR322-based plasmid vector pBMSF7C contained the ATI/p7.5 hybrid promoter within the hemagglutinin gene region of the vaccinia virus, which was reconstructed from the pSFJ1-10 plasmid and pBM vector [41,42]. Separate full-length cDNAs encoding either the HCV structural protein, nonstructural protein, or all HCV proteins were cloned from HCV R6 strain (genotype 1b) RNA by RT-PCR. Each cDNA was inserted into a separate pBMSF7C vector downstream of the pBMSF7C ATI/p7.5 hybrid promoter; the final designation of each recombinant plasmid was pBMSF7C-CN2, pBMSF7C-N25, or pBMSF-CN5 (Figure 2). They were then transfected into primary rabbit kidney cells infected with LC16m8 (multiplicity of infection = 10). The virus–cell mixture was harvested 24 h after the initial transfection by scrapping; the mixture was then frozen at −80°C until use. The hemagglutinin-negative recombinant viruses were cloned as previously described [42] and named rVV-CN2, rVV-N25, or rVV-CN5. Insertion of the HCV protein genes into the LC16m8 genome was confirmed by direct PCR, and expression of each protein from the recombinant viruses was confirmed by western blot analysis. The titers of rVV-CN2, rVV-N25, and rVV-CN5 were determined using a standard plaque assay and RK13 cells.

Statistical Analysis

Data are shown as mean ± SD. Data were analyzed using the nonparametric Mann–Whitney or Kruskal–Wallis tests or ANOVA as appropriate; GraphPad Prism 5 for Macintosh (GraphPad) was used for all analyses. P values <0.05 were considered statistically significant.

Supporting Information

Figure S1 HAI score of liver samples taken from CN2-29$^{(+/-)}$/MxCre$^{(+/-)}$ mice.
(EPS)

Figure S2 Lipid degeneration in samples of liver taken from CN2-29$^{(+/-)}$/MxCre$^{(+/-)}$ mice.
(EPS)

Figure S3 HCV protein expression after infection of LC16m8, rVV-CN2, rVV-N25, or rVV-CN5 into HepG2 cells.
(EPS)

Figure S4 Effects of treatment with rVV-N25 in RzCN5-15$^{(+/-)}$/MxCre$^{(+/-)}$ mice.
(EPS)

Figure S5 Daily cytokine profiles of the serum from CN2-29$^{(+/-)}$/MxCre$^{(+/-)}$ mice during the week following inoculation with LC16m8, rVV-CN2, rVV-N25, or rVV-CN5.
(EPS)

Figure S6 The immune response following poly(I:C) injection in the acute phase.
(EPS)

Figure S7 Detection of vaccinia virus DNA in the skin, liver, and spleen after inoculation with attenuated vaccinia virus (Lister strain) or highly attenuated vaccinia virus (LC16m8 strain).
(EPS)

Table S1 Incidence of hepatocellular carcinoma in male and female transgenic mice at 360, 480, and 600 days after poly(I:C) injection.
(EPS)

Text S1 Supporting information including material and methods, and references.
(DOCX)

Acknowledgments

We thank Dr. Fukashi Murai for supporting this study. We also thank Dr. Keiji Tanaka for providing the MxCre mice, Dr. Shigeo Koyasu for providing the GK1.5 (anti-CD4) and 53–6.72 (anti-CD8) monoclonal antibodies, and Dr Takashi Tokuhisa for helpful discussions.

Author Contributions

Performed the experiments: SS KK TC Y. Tobita TO FY Y. Tokunaga. Analyzed the data: SS KK TC MK. Contributed reagents/materials/analysis tools: KT-K TW TT MM K. Mizuno YH TH K. Matsushima. Wrote the paper: SS KK MK. Study concept and design: MK.

References

1. Lauer GM, Walker BD (2001) Hepatitis C virus infection. N Engl J Med 345: 41–52.
2. Alter MJ (1995) Epidemiology of hepatitis C in the West. Semin Liver Dis 15: 5–14.
3. Kawamura T, Furusaka A, Koziel MJ, Chung RT, Wang TC, et al. (1997) Transgenic expression of hepatitis C virus structural proteins in the mouse. Hepatology 25: 1014–1021.
4. Moriya K, Fujie H, Shintani Y, Yotsuyanagi H, Tsutsumi T, et al. (1998) The core protein of hepatitis C virus induces hepatocellular carcinoma in transgenic mice. Nat Med 4: 1065–1067.
5. Wakita T, Katsume A, Kato J, Taya C, Yonekawa H, et al. (2000) Possible role of cytotoxic T cells in acute liver injury in hepatitis C virus cDNA transgenic mice mediated by Cre/loxP system. J Med Virol 62: 308–317.
6. Wakita T, Taya C, Katsume A, Kato J, Yonekawa H, et al. (1998) Efficient conditional transgene expression in hepatitis C virus cDNA transgenic mice mediated by the Cre/loxP system. J Biol Chem 273: 9001–9006.
7. Folgori A, Capone S, Ruggeri L, Meola A, Sporeno E, et al. (2006) A T-cell HCV vaccine eliciting effective immunity against heterologous virus challenge in chimpanzees. Nat Med 12: 190–197.
8. Chisari FV, Ferrari C (1995) Hepatitis B virus immunopathology. Springer Semin Immunopathol 17: 261–281.
9. Machida K, Tsukiyama-Kohara K, Seike E, Tone S, Shibasaki F, et al. (2001) Inhibition of cytochrome c release in Fas-mediated signaling pathway in transgenic mice induced to express hepatitis C viral proteins. J Biol Chem 276: 12140–12146.
10. Kuhn R, Schwenk F, Aguet M, Rajewsky K (1995) Inducible gene targeting in mice. Science 269: 1427–1429.
11. Li K, Chen Z, Kato N, Gale M Jr, Lemon SM (2005) Distinct poly(I-C) and virus-activated signaling pathways leading to interferon-beta production in hepatocytes. J Biol Chem 280: 16739–16747.
12. Sugimoto M, Yamanouchi K (1994) Characteristics of an attenuated vaccinia virus strain, LC16m0, and its recombinant virus vaccines. Vaccine 12: 675–681.
13. Youn JW, Hu YW, Tricoche N, Pfahler W, Shata MT, et al. (2008) Evidence for protection against chronic hepatitis C virus infection in chimpanzees by immunization with replicating recombinant vaccinia virus. J Virol 82: 10896–10905.
14. Guidotti LG, Rochford R, Chung J, Shapiro M, Purcell R, et al. (1999) Viral clearance without destruction of infected cells during acute HBV infection. Science 284: 825–829.
15. Burkett MW, Shafer-Weaver KA, Strobl S, Baseler M, Malyguine A (2005) A novel flow cytometric assay for evaluating cell-mediated cytotoxicity. J Immunother 28: 396–402.

16. Pasquinelli C, Shoenberger JM, Chung J, Chang KM, Guidotti LG, et al. (1997) Hepatitis C virus core and E2 protein expression in transgenic mice. Hepatology 25: 719–727.
17. Lerat H, Honda M, Beard MR, Loesch K, Sun J, et al. (2002) Steatosis and liver cancer in transgenic mice expressing the structural and nonstructural proteins of hepatitis C virus. Gastroenterology 122: 352–365.
18. Lang KS, Georgiev P, Recher M, Navarini AA, Bergthaler A, et al. (2006) Immunoprivileged status of the liver is controlled by Toll-like receptor 3 signaling. The Journal of clinical investigation 116: 2456–2463.
19. Jasani B, Navabi H, Adams M (2009) Ampligen: a potential toll-like 3 receptor adjuvant for immunotherapy of cancer. Vaccine 27: 3401–3404.
20. Elmowalid GA, Qiao M, Jeong SH, Borg BB, Baumert TF, et al. (2007) Immunization with hepatitis C virus-like particles results in control of hepatitis C virus infection in chimpanzees. Proc Natl Acad Sci U S A 104: 8427–8432.
21. Satoi J, Murata K, Lechmann M, Manickan E, Zhang Z, et al. (2001) Genetic immunization of wild-type and hepatitis C virus transgenic mice reveals a hierarchy of cellular immune response and tolerance induction against hepatitis C virus structural proteins. J Virol 75: 12121–12127.
22. Crispe IN (2009) The liver as a lymphoid organ. Annu Rev Immunol 27: 147–163.
23. Chisari FV (2005) Unscrambling hepatitis C virus-host interactions. Nature 436: 930–932.
24. Saito T, Sherman GJ, Kurokohchi K, Guo ZP, Donets M, et al. (1997) Plasmid DNA-based immunization for hepatitis C virus structural proteins: immune responses in mice. Gastroenterology 112: 1321–1330.
25. Large MK, Kittlesen DJ, Hahn YS (1999) Suppression of host immune response by the core protein of hepatitis C virus: possible implications for hepatitis C virus persistence. Journal of immunology 162: 931–938.
26. Dustin LB, Rice CM (2007) Flying under the radar: the immunobiology of hepatitis C. Annu Rev Immunol 25: 71–99.
27. Bowie A, Kiss-Toth E, Symons JA, Smith GL, Dower SK, et al. (2000) A46R and A52R from vaccinia virus are antagonists of host IL-1 and toll-like receptor signaling. Proc Natl Acad Sci U S A 97: 10162–10167.
28. Zhu J, Martinez J, Huang X, Yang Y (2007) Innate immunity against vaccinia virus is mediated by TLR2 and requires TLR-independent production of IFN-beta. Blood 109: 619–625.
29. Samuelsson C, Hausmann J, Lauterbach H, Schmidt M, Akira S, et al. (2008) Survival of lethal poxvirus infection in mice depends on TLR9, and therapeutic vaccination provides protection. J Clin Invest 118: 1776–1784.
30. Sheikh MY, Choi J, Qadri I, Friedman JE, Sanyal AJ (2008) Hepatitis C virus infection: molecular pathways to metabolic syndrome. Hepatology 47: 2127–2133.
31. Tilg H, Moschen AR, Kaser A, Pines A, Dotan I (2008) Gut, inflammation and osteoporosis: basic and clinical concepts. Gut 57: 684–694.
32. Malaguarnera M, Di Fazio I, Laurino A, Ferlito L, Romano M, et al. (1997) Serum interleukin 6 concentrations in chronic hepatitis C patients before and after interferon-alpha treatment. Int J Clin Pharmacol Ther 35: 385–388.
33. Larrea E, Garcia N, Qian C, Civeira MP, Prieto J (1996) Tumor necrosis factor alpha gene expression and the response to interferon in chronic hepatitis C. Hepatology 23: 210–217.
34. Park EJ, Lee JH, Yu GY, He G, Ali SR, et al. (2010) Dietary and genetic obesity promote liver inflammation and tumorigenesis by enhancing IL-6 and TNF expression. Cell 140: 197–208.
35. Gregor MF, Hotamisligil GS (2011) Inflammatory mechanisms in obesity. Annu Rev Immunol 29: 415–445.
36. Humlova Z, Vokurka M, Esteban M, Melkova Z (2002) Vaccinia virus induces apoptosis of infected macrophages. The Journal of general virology 83: 2821–2832.
37. Choo QL, Kuo G, Weiner AJ, Overby LR, Bradley DW, et al. (1989) Isolation of a cDNA clone derived from a blood-borne non-A, non-B viral hepatitis genome. Science 244: 359–362.
38. Tsukiyama-Kohara K, Tone S, Maruyama I, Inoue K, Katsume A, et al. (2004) Activation of the CKI-CDK-Rb-E2F pathway in full genome hepatitis C virus-expressing cells. J Biol Chem 279: 14531–14541.
39. Nishimura T, Kohara M, Izumi K, Kasama Y, Hirata Y, et al. (2009) Hepatitis C virus impairs p53 via persistent overexpression of 3beta-hydroxysterol Delta24-reductase. J Biol Chem 284: 36442–36452.
40. Shimizu YK, Purcell RH, Yoshikura H (1993) Correlation between the infectivity of hepatitis C virus in vivo and its infectivity in vitro. Proc Natl Acad Sci U S A 90: 6037–6041.
41. Yasui F, Kai C, Kitabatake M, Inoue S, Yoneda M, et al. (2008) Prior immunization with severe acute respiratory syndrome (SARS)-associated coronavirus (SARS-CoV) nucleocapsid protein causes severe pneumonia in mice infected with SARS-CoV. J Immunol 181: 6337–6348.
42. Kitabatake M, Inoue S, Yasui F, Yokochi S, Arai M, et al. (2007) SARS-CoV spike protein-expressing recombinant vaccinia virus efficiently induces neutralizing antibodies in rabbits pre-immunized with vaccinia virus. Vaccine 25: 630–637.

RESEARCH PAPER

OncoImmunology 1:5, 581-592; August 2012; © 2012 Landes Bioscience

Cross-priming for antitumor CTL induced by soluble Ag + polyI:C depends on the TICAM-1 pathway in mouse CD11c$^+$/CD8α^+ dendritic cells

Masahiro Azuma, Takashi Ebihara,† Hiroyuki Oshiumi, Misako Matsumoto and Tsukasa Seya*

Department of Microbiology and Immunology; Hokkaido University Graduate School of Medicine; Sapporo, Japan

†Current affiliation: Howard Hughes Medical Institute; Washington University School of Medicine; St. Louis, MO USA

Keywords: cross-presentation, dendritic cell, TLR3, TICAM-1 (TRIF), tumoricidal CTL

Abbreviations: APC, antigen-presenting cells; CTL, cytotoxic T lymphocytes; DAMP, damage-associated molecular pattern; DC, dendritic cells; IFN, interferon; IPS-1, IFNβ promoter stimulator-1; MDA5, melanoma differentiation associated gene 5; Mf, macrophages; NK, natural killer; OVA, ovalbumin; PAMP, pathogen-associated molecular pattern; PRR, pattern-recognition receptors; PV, poliovirus; RIG-I, retinoic acid inducible gene-1; SL8, an OVA tetramer; TICAM-1, Toll-IL-1 receptor homology domain-containing molecule-1; TLR, Toll-like receptor; WT, wild-type

PolyI:C is a nucleotide pattern molecule that induces cross-presentation of foreign Ag in myeloid dendritic cells (DC) and MHC Class I-dependent proliferation of cytotoxic T lymphocytes (CTL). DC (BM or spleen CD8α$^+$) have sensors for dsRNA including polyI:C to signal facilitating cross-presentation. Endosomal TLR3 and cytoplasmic RIG-I/MDA5 are reportedly responsible for polyI:C sensing and presumed to deliver signal for cross-presentation via TICAM-1 (TRIF) and IPS-1 (MAVS, Cardif, VISA) adaptors, respectively. In fact, when tumor-associated Ag (TAA) was simultaneously taken up with polyI:C in DC, the DC cross-primed CTL specific to the TAA in a syngenic mouse model. Here we tested which of the TICAM-1 or IPS-1 pathway participate in cross-presentation of tumor-associated soluble Ag and retardation of tumor growth in the setting with a syngeneic tumor implant system, EG7/C57BL6, and exogenously challenged soluble Ag (EG7 lysate) and polyI:C. When EG7 lysate and polyI:C were subcutaneously injected in tumor-bearing mice, EG7 tumor growth retardation was observed in wild-type and to a lesser extent IPS-1$^{-/-}$ mice, but not TICAM-1$^{-/-}$ mice. IRF-3/7 were essential but IPS-1 and type I IFN were minimally involved in the polyI:C-mediated CTL proliferation. Although both TICAM-1 and IPS-1 contributed to CD86/CD40 upregulation in CD8α$^+$ DC, H2K^b-SL8 tetramer and OT-1 proliferation assays indicated that OVA-recognizing CD8 T cells predominantly proliferated in vivo through TICAM-1 and CD8α$^+$ DC is crucial in ex vivo analysis. Ultimately, tumor regresses > 8 d post polyI:C administration. The results infer that soluble tumor Ag induces tumor growth retardation, i.e., therapeutic potential, if the TICAM-1 signal coincidentally occurs in CD8α$^+$ DC around the tumor.

Introduction

Cytotoxic T lymphocytes (CTL) and natural killer (NK) cells are two major effectors for antitumor cellular immunity. These effectors are driven through activation of dendritic cells (DC) and/or macrophages (Mf), which is mediated by pattern-recognition receptors (PRRs) for the recognition of microbial patterns.[1,2] Antigen (Ag) presentation and upregulation of NK cell-activating ligands are major events induced in DC/Mf in response to PRRs, which link to evoking CTL- and NK-antitumor immunity, respectively. The immune-potentiating function of specific components of the classical adjuvants are largely attributable to the ligand activity of PRRs (CpG DNA/TLR9, polyI:C/TLR3, monophosphoryl lipid (MPL) A/TLR4, Pam2/TLR2, etc.).[3] That is, the DC/Mf competent to drive effectors are generated through PRR signal in inflammatory nest where affected cells and recruited immune cells encounter exogenous or endogenous PRR ligands. Since studying the functional properties of PRRs in tumor immunity is on the way using a variety of possible ligands and cell biological analyses, immune responses reflecting the total adjuvant potential around Ag-presenting cells (APC) in local inflammatory nests are not always elucidated even in mice.

RNA-sensing PRR pathways, including TLR3-TICAM-1, TLR7-MyD88 and RIG-I/MDA5-IPS-1 participate in driving Type I IFN induction and cellular immunity in DC subsets.[1,4,5] Type I IFN and the IFNAR pathway in DC and other cells reportedly evoke and amplify T cell immunity.[5,6] TLR7 resides exclusively in plasmacytoid DC[7] whereas TLR3 mainly exists in

*Correspondence to: Tsukasa Seya; Email: seya-tu@pop.med.hokudai.ac.jp
Submitted: 02/04/12; Revised: 03/02/12; Accepted: 03/02/12
http://dx.doi.org/10.4161/onci.19893

myeloid DC/Mf and epithelial cells.[8] They are localized on the membrane of the endosome and deliver the signal via their adaptors, MyD88 and TICAM-1.[7,8] RIG-I and MDA5 are ubiquitously distributed to a variety of mouse cells and signal the presence of cytoplasmic viral products through IPS-1.[9] Thus, TLR3 and RIG-I/MDA5 are candidates associated with DC maturation to drive effector cells.[10] Indeed, viral dsRNA analog, polyI:C, is a representative ligand for TLR3 and MDA5 and induces polyI:C-mediated DC-NK reciprocal activation.[11,12] These are also true in human DC.[13]

The point of this study is by which pathway antitumor CTL are induced for tumor regression in a mouse tumor-implant model. It has been postulated that DC present exogenous tumor Ag to the MHC Class I-restricted Ag-presentation pathway and proliferate CD8 T cells specific to the extrinsic Ag. When tumor cells provide soluble and insoluble exogenous Ag, this Class I Ag presentation occurs mostly TAP/proteasome-dependent, suggesting the pathway partly sharing with that for endogenous Ag presentation. This DC's ability to deliver exogenous Ag to the pathway for MHC Class I-restricted Ag presentation has been described as cross-presentation.[14] DC cross-presentation leads to the cross-priming and proliferation of Ag-specific CD8 T cells in vivo and in vitro.[14-18] A variety of PAMP[15,16] and intrinsic DAMP[17] as well as other factors including Type I IFN,[5,18] $CD4^+$ T cells[19] and NKT cells[20] augment cross-priming in tumor-bearing mice. However, by what molecular mechanism polyI:C enhances CTL induction in tumor-bearing mice remains largely unsettled.

Here, we made an EG7 tumor-implant mouse system and treated the mice with s.c.-injected ovalbumin (OVA)-containing cell lysates (Ag) and polyI:C. Spleen $CD8\alpha^+$ DC turn CTL-inducible when stimulated with Ag and polyI:C. In either case of s.c., i.p., or i.v. injection of polyI:C, the TLR3/TICAM-1 pathway predominantly participates in $CD8\alpha^+$ DC cross-priming and antitumor CTL induction. Earlier studies using non-tumor models, suggested that both TLR3 and MDA5 appeared to participate in polyI:C-dependent CTL induction.[21] TLR3 is predominantly involved in primary Ag response and Th1 skewing,[22] while MDA5 participates in secondary Ag response.[23] Importance of TLR3 in induction of cross-priming was first suggested by Schulz et al., who used OVA/polyI:C-loaded or virus-infected xenogenic (Vero) cells and mouse DC.[16] Here we demonstrate that the antitumor polyI:C activity is sustained by the TICAM-1 pathway in any route of injection in tumor-implant mice: antitumor CTL responses are mostly abrogated in TICAM-$1^{-/-}$ but not IPS-$1^{-/-}$ mice.

Results

Properties of EG7 tumor with high MHC in tumor-loading mice. The properties of the EG7 line we used are consistent with those reported previously.[24,25] It expressed high MHC Class I (H2-Kb) and no Qa-1b or Rae-1 (**Fig. S1**). The expression levels of these proteins were barely changed before and after implantation of EG7 cells into mice. Cell viability was not affected by in vitro stimulation with polyI:C only (**Fig. S1B**). However, a batch-to-batch difference of cell viability may have affected the rate of tumor growth in each mouse tumor-implant experiment.

$CD8^+$ T cells are responsible for tumor retardation by polyI:C. EG7 cells (2×10^6) were inoculated into the back of C57BL/6 (WT), and the indicated reagents were subcutaneously (s.c.) injected around the EG7 tumor (**Fig. 1A**). Growth retardation of tumor was observed by treatment with polyI:C or polyI:C plus EG7 lysate (**Fig. 1A**). EG7 lysate only had no effect on tumor regression. When $CD8\beta^+$ T cells were depleted before EG7 lysate/polyI:C treatment, polyI:C-mediated tumor growth suppression was cancelled (**Fig. 1A**), suggesting the participation of CD8 T cells in tumor growth suppression. The therapeutic potential of polyI:C appeared to be more reproducible in the presence of EG7 lysate than in the absence, judged from the increases of activated $CD8^+$ T cells (**Fig. 1B**) and cytotoxic activity (**Fig. 1C**) of LN T cells isolated from the mice sacrificed after the last therapy. Yet, the EG7 Ag could be more or less supplied from the implant tumor. $NK1.1^+$ cells did not participate in this EG7 tumor regression in this setting (data not shown).

Since EG7 lysate contains OVA, OVA-specific T cells in draining LN and spleen of the WT mice were counted by tetramer assay after the last therapy (**Fig. S2A and B**). The numbers of tetramer-positive cells were prominently increased in LN and spleen in mice with EG7 lysate and polyI:C. We confirmed the importance of simultaneous administration of Ag plus polyI:C for OVA-specific CTL induction as in **Figure S2C**, where pure Ag (OVA) was used instead of EG7 lysate for immunotherapy. The polyI:C adjuvant function appeared to be more efficient in the mixture of pure Ag than in polyI:C alone. Tumor regression (**Fig. S2C**) and OVA-specific CTL induction (**Fig. S2D**) were clearly observed in this additional experiment. To obtain reproducible data, we employed the EG7 lysate/polyI:C combination therapy as follows.

IFN-inducing pathways are involved in PolyI:C-derived EG7 growth retardation. We next inoculated EG7 cells (2×10^6) into the back of C57BL/6 (WT), TICAM-$1^{-/-}$, IPS-$1^{-/-}$, or TICAM-1/IPS-1 double-deficient (DKO) mice (**Fig. 2**). We s.c. administered EG7 lysate with or without polyI:C around the tumor. The EG7 lysate was the soluble fraction of EG7 which removed insoluble debris by centrifugation. The EG7 lysate contained unprecipitated micro-debris and soluble Ag. No other emulsified reagent was added for immunization. Thus, the adjuvant function of polyI:C per se is reflected in the tumor growth, although polyI:C had to be injected into mice twice a week. Retardation of tumor growth was observed $>$ 8 d after immunization with EG7 lysate + polyI:C in WT mice, though no growth retardation without polyI:C (**Fig. 2A**). The polyI:C-mediated tumor growth suppression was largely abrogated in TICAM-$1^{-/-}$ (**Fig. 2B**) and to a lesser extent in IPS-$1^{-/-}$ mice (**Fig. 2C**), and completely in TICAM-1/IPS-1 DKO mice (**Fig. 2D**). Hence, TICAM-1 plays an important role in inducing polyI:C-mediated tumor growth retardation in the s.c. setting we employed.

CD8 T cell activation induced by the TICAM-1 pathway. CD8 T cell activation in the inguinal LN was tested with polyI:C + EG7 lysate in EG7 tumor-bearing mice using CD69 as

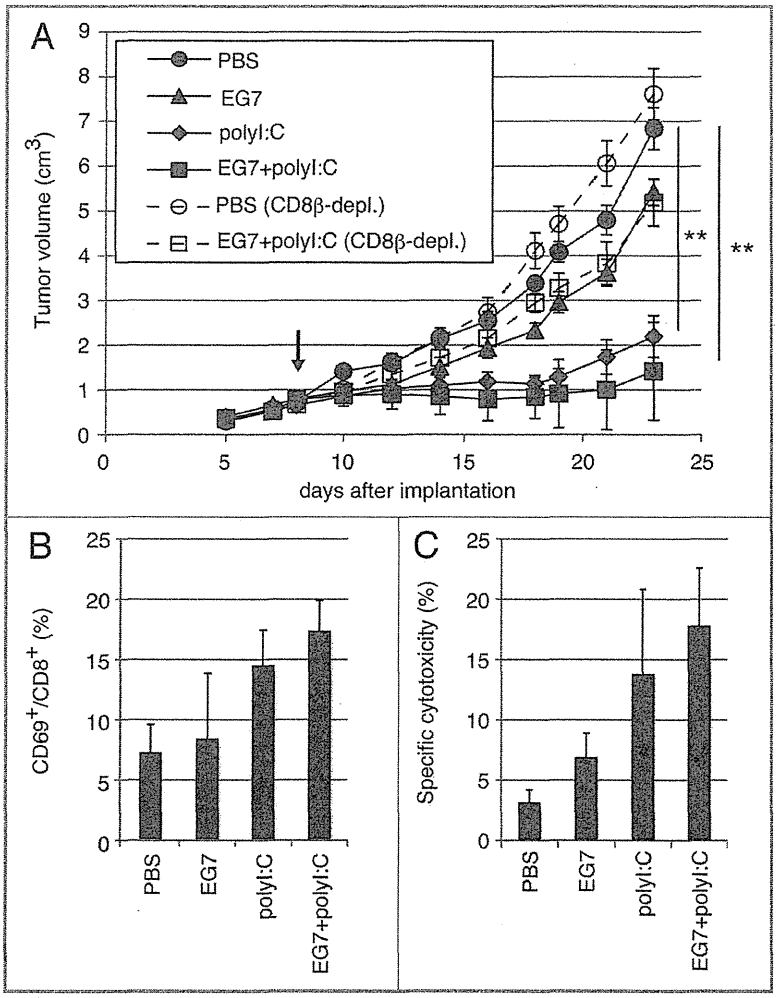

Figure 1. PolyI:C induces CTL-mediated tumor regression. (A) WT mice were challenged with EG7 cells and were treated with PBS (●), EG7 lysates (▲), polyI:C (◆) and EG7 lysates + polyI:C (■). The adjuvant therapy was started at the time indicated by the arrow and the indicated reagents injected twice per week. One of the two PBS groups (○) and one of the two EG7 lysates + polyI:C groups (□) were treated with anti-CD8β ascites in order to deplete $CD8^+$ T cells once a week. Each group had 3–5 mice. (B) Draining inguinal LNs were harvested 24 h after the last treatment and the proportion of CD69-expressing $CD8^+$ cells were counted. (C) LN cells were co-cultured with MMC-treated EG7 cells for 3 d and subjected to ^{51}Cr release assay to evaluate CTL activity. E/T = 50. All error bars used in this figure show ± SEM. Data are representative of two independent experiments. One-way analysis of variance (ANOVA) with Bonferroni's test was performed to analyze statistical significance. **, $p < 0.01$.

an activating marker. Twenty-four hours after the last polyI:C + EG7 sec.c. treatment, cells were harvested from the LN excised (**Fig. 3A**). FACS profiles of total cells from each mouse group are shown in **Fig. S3**. By combination therapy with EG7 lysate and polyI:C, T cells were activated in WT and IPS-$1^{-/-}$ mice, but the proportion of CD8 T cells was not affected by the therapy (**Fig. S4A**). Under the same conditions, T cells were barely activated in TICAM-$1^{-/-}$ mice in response to polyI:C (**Fig. 3A**). The proportion of $CD69^+$ cells are indicated in **Figure 3B**. IL-2 (**Fig. 3C**) and IFNγ (**Fig. S4B**) were highly induced in the WT and IPS-$1^{-/-}$ LN cells, while they were not induced in TICAM-$1^{-/-}$ or DKO cells. IFNγ levels were upregulated only in polyI:C-treated tumor-bearing mice, although the WT > IPS-$1^{-/-}$ profile for IFNγ production was reproducibly observed (**Fig. S4B**).

In vivo proliferation of CD8 T cells judged by tetramer assay and IFNγ induction. We next tested whether i.p. injection of polyI:C plus OVA induces CTL proliferation. PolyI:C and OVA were i.p. injected into mice and the polyI:C-dependent cross-priming of CD8 T cells were examined using the OVA tetramer assay. OVA-specific CD8 T cells were clonally proliferated in WT and IPS-$1^{-/-}$ mice, but not in TICAM-1/IPS-1 DKO and IRF-$3/7^{-/-}$ mice (**Fig. 4A**). Proliferation of OVA-specific CD8 T cells were severely suppressed in TICAM-$1^{-/-}$ mice (**Fig. 4A**), suggesting that polyI:C-mediated cross-priming of CD8 T cells largely depends on the TICAM-1 pathway followed by IRF-3/7 activation in the i.p. route. The results were reproduced in additional experiments using more mice (**Fig. 4B**) and TLR$3^{-/-}$ mice (**Fig. S5A and B**). The polyI:C cytokine response, where IFNα is IPS-1-dependent while IL-12p40 is TICAM-1-dependent, was also confirmed in serum level by polyI:C i.p. injection (**Fig. S5E**). Specific induction of IFNγ (**Fig. 4C**) was also observed in parallel with the results of **Figure 4A**.

Whether or not i.v. injection of polyI:C plus OVA induces Ag-specific CTL and cytotoxicity was next checked. OVA-specific OT-1 proliferation and cytotoxicity (**Fig. 4D and E**) were observed in in vivo analyses of WT and IPS-$1^{-/-}$ CD8 T cells but not of TICAM-$1^{-/-}$, TICAM-1/IPS-1 DKO, and IRF-$3/7^{-/-}$ mice in the i.v. setting.

Since TICAM-1 is the adaptor for TLR3 as well as cytoplasmic helicases,[24] we confirmed the level of cross-priming being decreased in TLR$3^{-/-}$ mice and an expected result was obtained (**Fig. S5A and B**). Furthermore, in IFNAR$^{-/-}$ mice, OVA-specific CTL induction was slightly reduced compared with that in WT mice, but higher than in TICAM-$1^{-/-}$ mice (**Fig. S5C and D**). Hence, in vivo cross-presentation induced by polyI:C mostly depends on the TLR3-TICAM-1 pathway followed by transcriptional regulation by IRF-3/7 in any administration route, and is further promoted by Type I IFN presumably produced by the stromal cells through the IPS-1 pathway.[26]

IPS-1 induces DC maturation but not cross-priming in vivo. Spleen DC maturation by i.v.-injected polyI:C was tested ex vivo using $CD8\alpha^+$ DC and $CD8\alpha^-$ DC isolated from WT or KO mice with no tumor as indicated in **Figure 5A**. The maturation markers CD86 and CD40 were upregulated on both $CD8\alpha^+$ and $CD8\alpha^-$

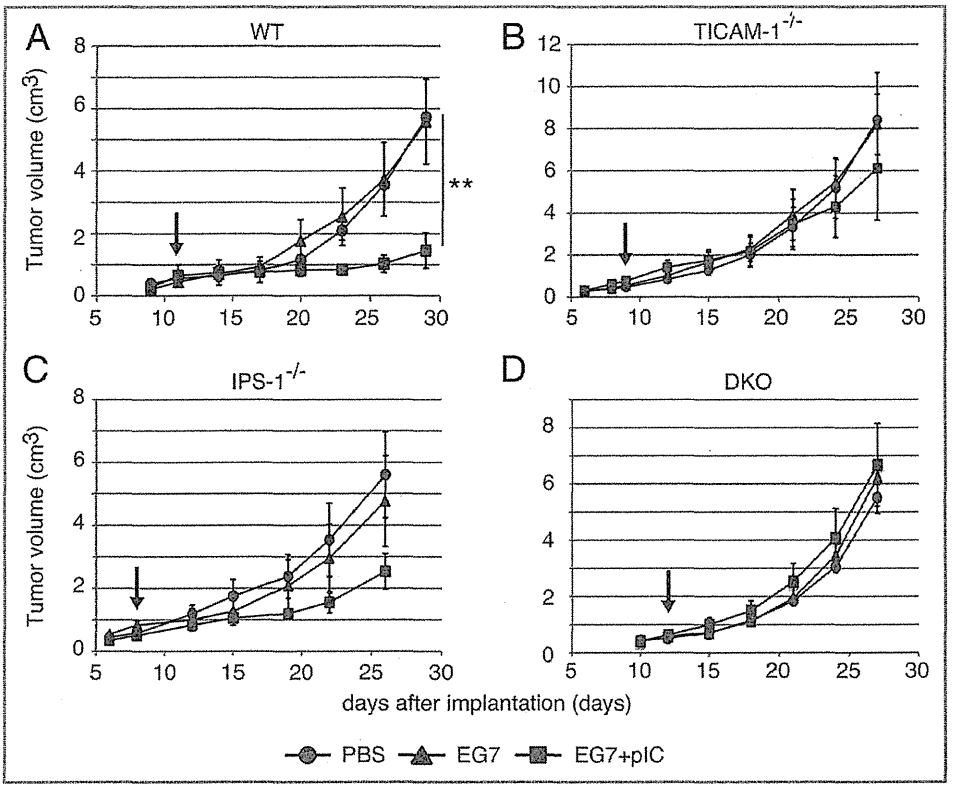

Figure 2. PolyI:C-induced tumor retardation is dependent on the TICAM-1 pathway. Antitumor effect of polyI:C on various KO mice were evaluated by using in vivo mouse tumor implant model. EG7 cells were inoculated to WT (A), TICAM-1$^{-/-}$ (B), IPS-1$^{-/-}$ (C) and DKO mice (D) on day 0. PBS (●), EG7 lysates (▲) or EG7 lysates + polyI:C (■) were s.c. administered around the tumor. The adjuvant therapies were started at the time indicated by the arrows and injected twice per week. Each group have 3–4 mice and error bar shows ± SEM. Data are representative of two independent experiments. **, $p < 0.01$

DC from WT mice when they were stimulated with OVA and polyI:C. Treatment of DC with OVA only did not induce upregulation of CD86 and CD40. Although the expression levels of CD86 and CD40 were a little less in CD8α$^+$ and CD8α$^-$ DC from TICAM-1$^{-/-}$ or IPS-1$^{-/-}$ mice than those from WT mice, both CD86 and CD40 were sufficiently upregulated even in the abrogation of either one pathway in polyI:C-injected mice. The CD86 and CD40 shifts were completely abolished in DKO mice (**Fig. 5A**). Thus, the TICAM-1 pathway participates in both potent co-stimulation and cross-priming, while the IPS-1 pathway mainly participates only in integral co-stimulation in myeloid DC.

We next assessed in vitro proliferation of OT-1 cells. CD8α$^+$ and CD8α$^-$ DC were prepared from PBS, polyI:C, OVA and OVA/polyI:C-treated mice, and mixed in vitro with CFSE-labeled OT-1 cells. WT, TICAM-1$^{-/-}$ and IPS-1$^{-/-}$ mice were used for this study. OT-1 proliferation was observed with CD8α$^+$ DC but not CD8α$^-$ DC when OVA + polyI:C was injected (**Fig. 5B**). Furthermore, the OT-1 proliferation barely occurred in the mixture containing TICAM-1$^{-/-}$ CD8α$^+$ DC. Thus, OT-1 proliferation is triggered by the TICAM-1 pathway in CD8α$^+$ DC. Again, IPS-1 had almost no effect on OT-1 proliferation with CD8α$^+$ DC in this setting. In the mixture, IFNγ was produced in the supernatants of WT and IPS-1$^{-/-}$ CD8α$^+$ DC but not TICAM-1$^{-/-}$ DC by stimulation with OVA + polyI:C (**Fig. 5C**). No IFNγ was produced in the supernatants of CD8α$^-$ DC even from WT mice, which results are in parallel with those of OT-1 proliferation. In any case irrespective of tumor-bearing or not, Ag, polyI:C and the TICAM-1 pathway are mandatory for CD8α$^+$ DC to cross-prime and proliferate OVA-specific CD8 T cells.

We checked the TICAM-1- or IPS-1-specific gene expressions related to Type I IFN and MHC Class I presentation using genechip and qPCR (**Fig. S6**). PolyI:C-mediated upregulation of *Tap1*, *Tap2* and *Tapbp* messages diminished in TICAM-1$^{-/-}$ BMDC (**Fig. S6A**). The levels of these genes were hardly affected in IPS-1$^{-/-}$ BMDC (data not shown). PolyI:C-mediated upregulation was observed with MDA5 (*Ifih1*) in CD8α$^-$ and CD8α$^+$ DCs (**Fig. S6B**). Surprisingly, other factors including TLR3, TICAM-1 and MAVS messages were all downregulated in response to polyI:C in CD8α$^+$ DC (**Fig. S6B**), for the reason as yet unknown.

Effect of TLR3-mediated IFN-inducing pathway on anti-tumor CTL induction. PolyI:C is a dsRNA analog capable of incorporating into the endosome and cytoplasm by exogenous administration in vitro.[27,28] However, no evidence has been proposed that polyI:C is internalized into the endosome of

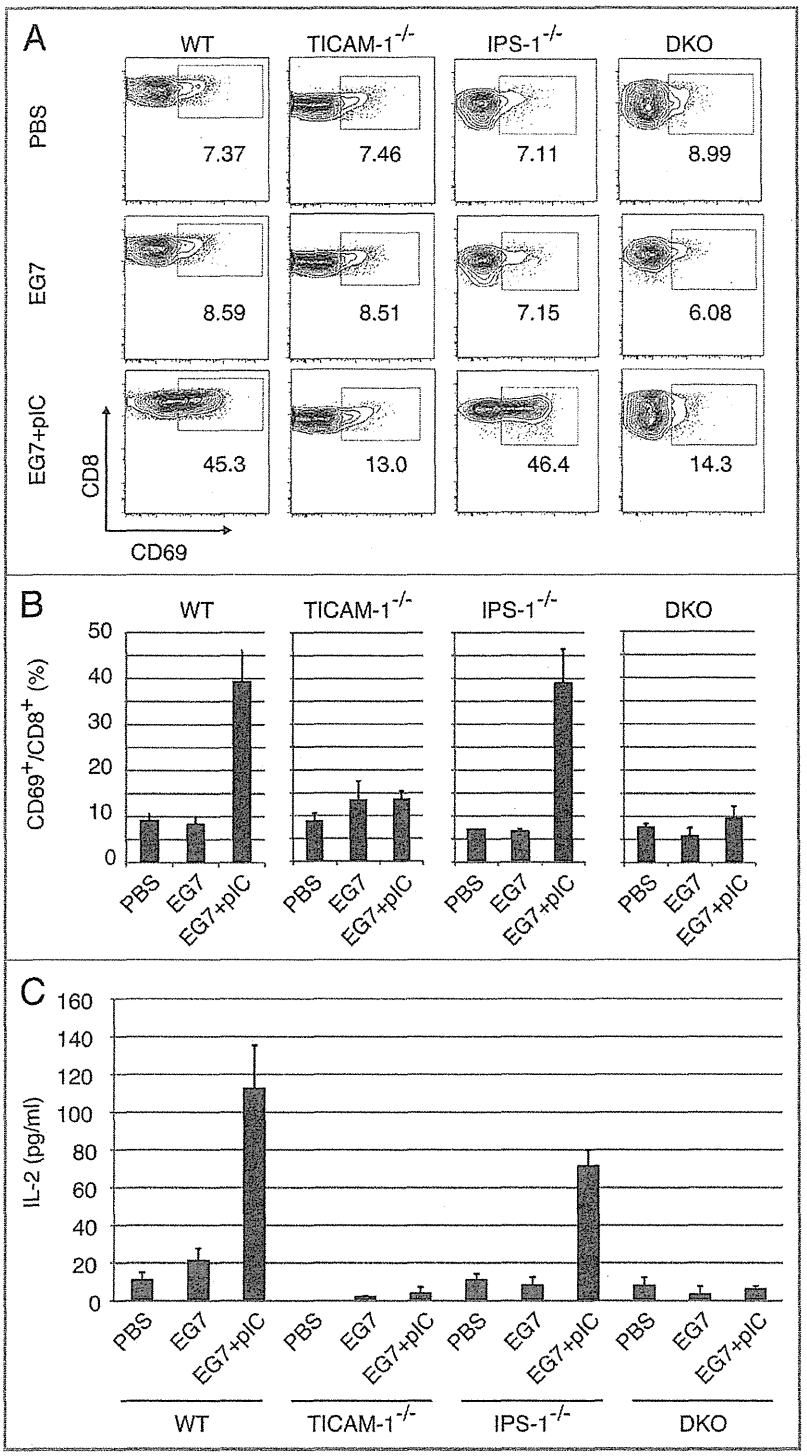

Figure 3. CD8 T cells in the draining LNs are activated through the TICAM-1 pathway by polyI:C. Draining inguinal LNs were harvested from tumor-bearing mice 24 h after the last treatment. LN cells were stained with CD3ε, CD8α and CD69, and the cells gated on $CD3\varepsilon^+CD8\alpha^+$ are shown (A). Spleen cells in each group of mice were stained separately, the CD8 levels in gated cells being variably distributed in FACS analyses. The average frequency of activated CD8 T cells defined by CD69 expression is shown (B). Alternatively, LN cells from the indicated mice were cultured for further 3 d in vitro and IL-2 production was measured by CBA assay (C).

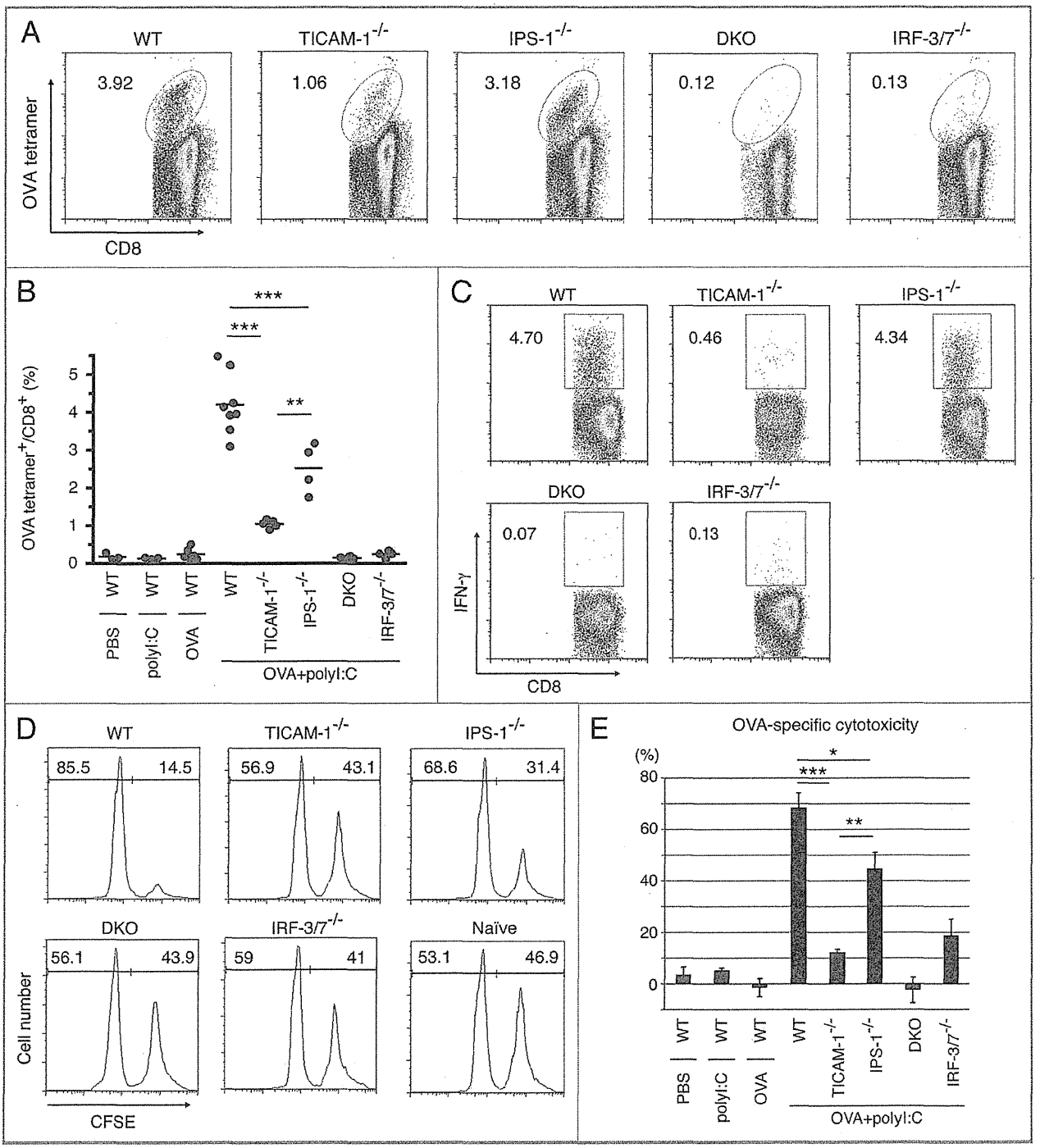

Figure 4. TICAM-1 and IRF-3/7 are essential for polyI:C-induced antigen-specific CTL expansion. WT, TICAM-1$^{-/-}$, IPS-1$^{-/-}$, TICAM-1/IPS-1 DKO and IRF-3/7$^{-/-}$ mice were i.p. administered with the combination of OVA and polyI:C. After 7days, splenocytes were harvested and stained with CD8α and OVA tetramer (A). The average percentages of OVA-specific CTL are shown (B). Alternatively, splenocytes were cultured in vitro in the presence of SL8 for 8 h and IFNγ production was measured by intracellular cytokine staining (C). To assess the killing activity, in vivo CTL assay was performed. The combinations of OVA and polyI:C were administered i.v. to each group of mice and 5 d later, cytotoxicity was measured (D). The data shown are collaborate or representative of at least three independent experiments. One-way analysis of variance (ANOVA) with Bonferroni's test was performed to analyze statistical significance. *, $p < 0.05$; **, $p < 0.01$; ***, $p < 0.001$.

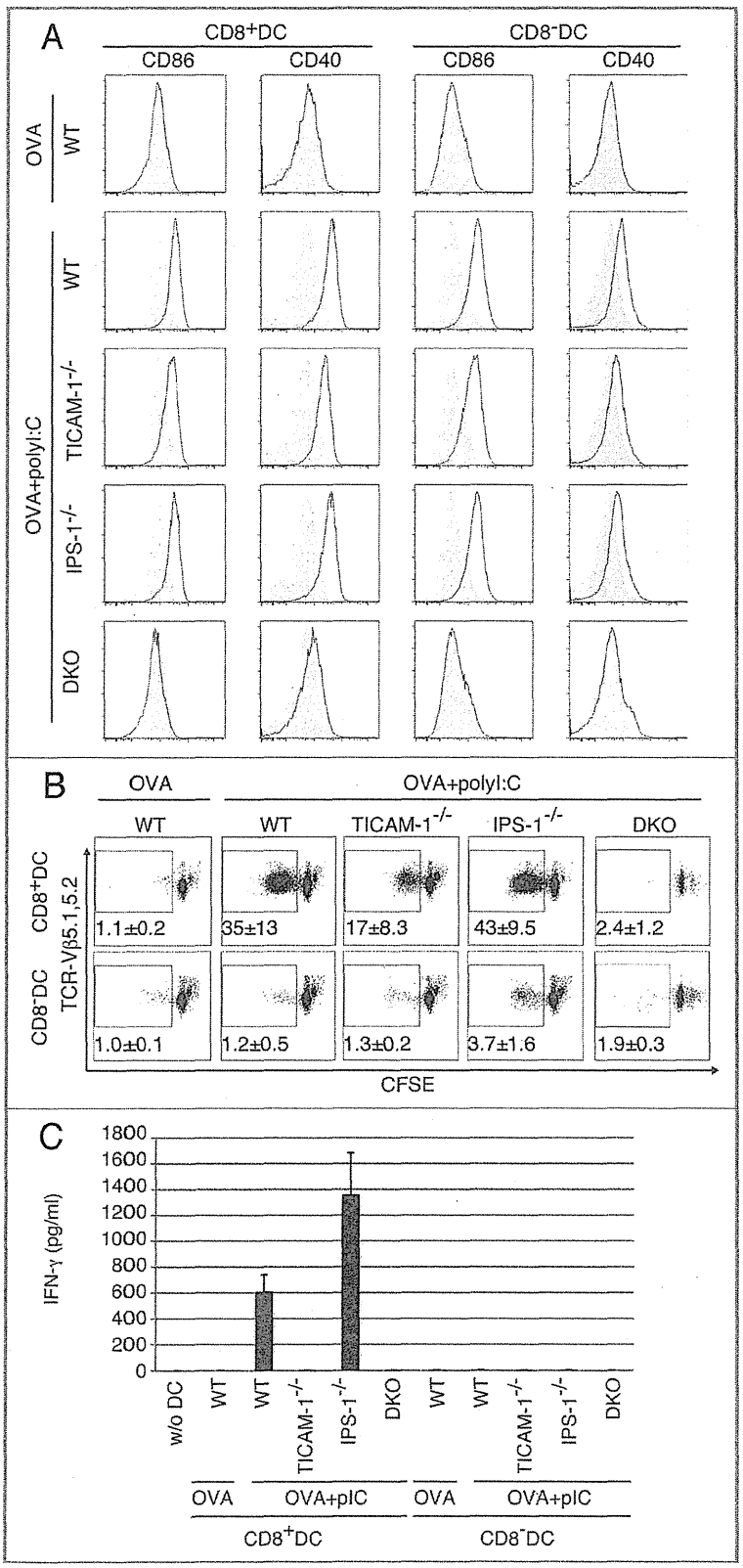

Figure 5. TICAM-1 in CD8α⁺ DC is more important than IPS-1 in polyI:C-induced cross-priming. OVA and polyI:C were administered i.v. and 4 h later, CD8α⁺ and CD8α⁻ DC were isolated from the spleen. CD86 and CD40 expressions were determined by FACS (A). Filled gray and black line show isotype control and target expression, respectively. Alternatively, CD8α⁺ and CD8α⁻ DC were co-cultured with CFSE-labeled RAG2$^{-/-}$/OT-1 T cells for 3 d. The cross-priming activity of each DC subset was determined with sequential dilution of CFSE (B) and IFNγ production (C). IFNγ was measured by CBA assay. The data shown are representative of two independent experiments. Err bar shows SD.

CD8α⁺ DC where TLR3 is expressed in vivo. Peritoneal (PEC) Mf and bone marrow-derived DC[22] usually phagocytoze polyI:C and deliver them into the endosome. In mouse CD8α⁺ DC direct internalization of polyI:C has remain unproven. Using labeled polyI:C and anti-mouse TLR3 mAb, 11F8,[22] we checked whether the exogenously-added polyI:C encountered with TLR3 in CD8α⁺ DC in vitro. TLR3 (green) was merged with TexasRed-polyI:C 30–120 min after polyI:C stimulation in the culture (**Fig. 6A**). The quantities of CD8α⁺ and CD8α⁻ DC where FITC-polyI:C was incorporated were determined by FACS analysis (**Fig. 6B**). Thus, the process by which polyI:C injected reaches the endosomal TLR3 is delineated in the CD8α⁺ DC.

Discussion

PolyI:C is an analog of virus dsRNA, and acts as a ligand for TLR3 and RIG-I/MDA5. PolyI:C has been utilized as an adjuvant for enhancement of antitumor immunity for a long time.[29] However, the mechanistic background of the therapeutic potentials of polyI:C against cancer has been poorly illustrated. It induces antitumor NK activation through DC-NK cell-to-cell interaction when CD8α⁺ DC TLR3 is stimulated in the spleen.[11] Besides myeloid cells, however, some tumor cell lines express TLR3 and dsRNA targeting tumor cells may affect the growth rate of tumors,[30] where the receptor-interacting protein (RIP) pathway is involved downstream of TICAM-1.[31] Here we showed evidence that polyI:C injection facilitates maturation of TLR3-positive CD8α⁺ DC (i.e., APC) to trigger CTL induction against exogenous soluble Ags including EG7 lysate or OVA. The TICAM-1 adaptor for TLR3 and IRF-3/7 are involved in the cross-presentation signal in CD8α⁺ DC, but the molecule/mechanism downstream of TICAM-1 that governs cross-presentation remains elusive. Since most of the tumor-associated Ags (TAA) are predicted to be liberated from tumor cells

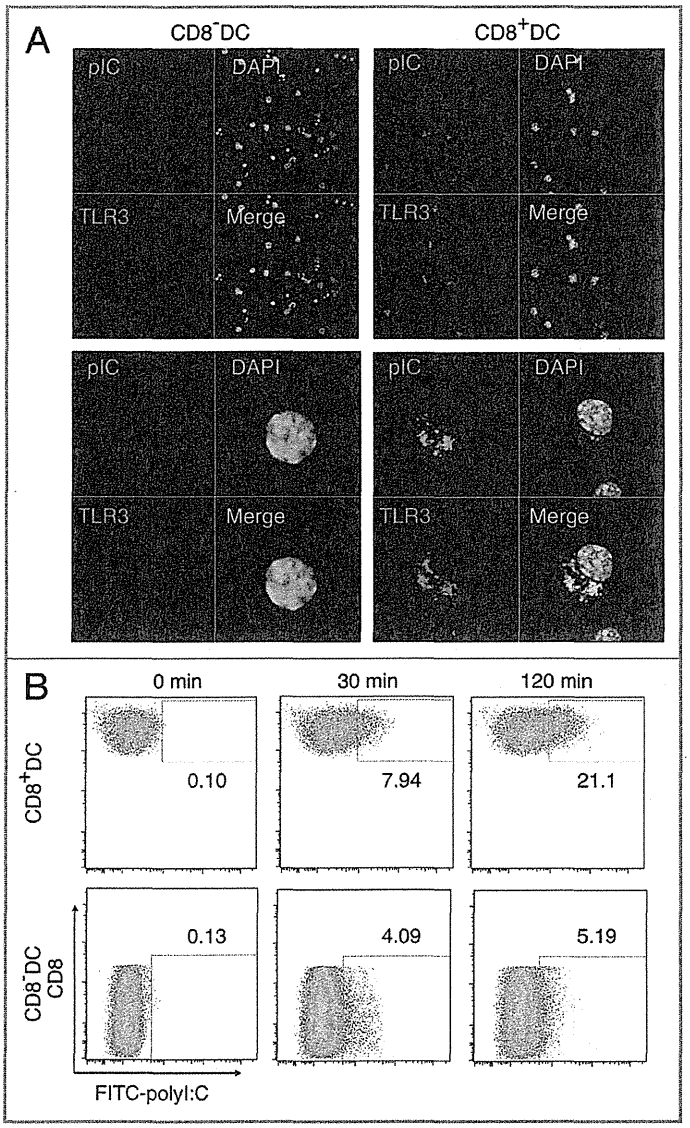

Figure 6. PolyI:C encounters TLR3 in CD8α⁺ DC. CD8α⁺ and CD8α⁻ DC were isolated by FACSAriaII and stimulated with 20 μg/ml TexasRed-polyI:C for 2 h. Then cells were stained with Alexa647-antiTLR3 and subjected to confocal microscopic analysis (A). Alternatively, splenic DC isolated by MACS were incubated with FITC-polyI:C for the time shown in figure and analyzed the degrees of polyI:C uptake by FACS (B). Data shown are the representative of three independent experiments.

as soluble Ags, the TICAM-1 pathway in CD8α⁺ DC would be crucial for driving of tumor-specific CTL around the tumor microenvironment. In any route of polyI:C injection, this is true as shown first in this study. Although TICAM-1 is an adaptor of other cytoplasmic sensors, DDX1, DDX21 and DHX36,[32] the antitumor CTL responses are merely relied on TLR3 of CD8α⁺DC in this system. Taken together with previous reports,[11,12] TICAM-1 signaling triggers not only NK activation but also CTL induction.

TLR3 and MDA5 are main sensors for dsRNA and differentially distributed in myeloid cells.[33,34] TLR3 is limitedly expressed in myeloid, epithelial and neuronal cells,[33] whereas MDA5 is ubiquitously expressed including non-myeloid stromal cells.[33] Several reports suggested that i.v. injection of polyI:C predominantly stimulate the stromal cells which express IFNAR,[26] thereby robust type I IFN are liberated from these cells to be a systemic response including cytokinemia and endotoxin-like shock.[35,36] Both TLR3 and MDA5 link to the IRF-3/7-activating kinases leading to the production of IFNα/β.[37,38] Once IFNα/β are released, IFNAR senses it to amplify the Type I IFN production,[39] and reportedly this amplification pathway involves cross-priming of CD8 T cells in viral infection.[18] Tumor progression or metastasis can be suppressed through the IFNAR pathway.[40] These scenarios may be right depending on the conditions employed. Our message is related to what signal pathway is fundamentally required for induction of antitumor CTL in DC. The CTL response is almost completely abrogated in TICAM-1$^{-/-}$ and IRF-3/7$^{-/-}$ mice, but largely remains in IPS-1$^{-/-}$ and IFNAR$^{-/-}$ mice when Ag and polyI:C are extrinsically administered. The results are reproducible in some other tumor-implant models (data not shown), and even in IFNAR$^{-/-}$ mice, TICAM-1-specific genes are upregulated to confer tumor cytotoxicity (**Fig. S6**, Azuma et al., unpublished data). In addition, the upregulation of these genes is independent of IPS-1 knockout in DC. Our results infer that the primary sensing of dsRNA in CD8α⁺ DC is competent to induce cross-presentation, which minimally involves the IPS-1 or IFNAR amplification pathway, at least at a low dose of polyI:C. Yet, subsequent induction of Type I IFN via the IFNAR may further amplify the cross-priming.[18,41] Further studies are needed as to which of the TICAM-1-inducible genes link to the cross-presentation in CD8α⁺ DC.

The main focus of this study was to identify the pathway for transversion of immature DC to the CTL-driving phenotype by co-administration of polyI:C with soluble Ag. The IPS-1 pathway, although barely participates in antitumor CTL driving, can upregulate CD40/CD86 co-stimulators on the membranes of splenic CD8α⁺ and CD8α⁻ DC in response to polyI:C, suggesting that MDA5 does function in the cytoplasm of splenic CD8α⁺ and CD8α⁻ DC to sense polyI:C. However, effective CTL induction happens only in CD8α⁺ DC when stimulated with polyI:C. CD8α⁺ DC express TLR3 but CD8α⁻ DC do not, and CD8α⁺ DC with no TLR3 fail to induce CTL, suggesting that integral co-stimulation by MDA5/IPS-1 is insufficient for DC to induce cross-priming of CD8 T cells: antitumor CTL are not induced until the TICAM-1 signal is provided in DC. At least, sole effect of the IPS-1 pathway and upregulation of co-stimulators on CD8α⁺ DC is limited for cross-priming and induction of antitumor CTL, which result partly reflects those in a previous report where IPS-1 and TICAM-1 harbor a similar potential for CD8 T cell proliferation when

polyI:C (Alum-containing) is employed as an adjuvant for CD8α+ DC to test proliferation of anti-OVA CTL.[21]

A question is why TICAM-1 is dominant to IPS-1 for response to exogenously-added polyI:C in CD8α+ DC. The answer is rooted in the difference of functional behavior between BMDC and CD8α+ DC. TLR3 levels are variable depending upon subsets of DC,[22] which affects DC subset-specific induction of cellular immune response. The high TLR3 expression (partly surface-expressed) is situated in CD8α+ DC before polyI:C stimulation, which is distinct from the properties of F4/80+ Mf and presumably BMDC of low TLR3 expression. The polyI:C-uptake machinery[15] appears to efficiently work in concert with the TLR3/TICAM-1 pathway in CD8α+ DC and this tendency is diminished when CD8α+ DC are pretreated with Alum + polyI:C.[21] Furthermore, there are functional discrepancies between CD8α+ splenic DC and GM-CSF-induced BMDC, which appears to reflect the difference of their TLR3 levels.[22] These results on CD8α+ DC encourage us to develop dsRNA adjuvant immunotherapy supporting TAA soluble vaccines for cancer applicable to humans, which possess the counterpart of CD8α+ DC.

There are two modes of dsRNA-mediated DC maturation, intrinsic and extrinsic modes that are governed by the IPS-1 and TICAM-1 pathways, respectively.[9,34] It is important to elucidate the in vivo qualitative difference in the two pathways in tumor-loading mice. TLR3+ DC/Mf are responsible for CTL driving via an extrinsic route in viral infection.[34] Previous data suggested that dsRNA in infectious cell debris, rather than viral dsRNA produced in the cytoplasm of Ag-presenting cells or autophagosome formation, contribute to fine tuning of DC maturation through extrinsic dsRNA recognition.[16] It is reported that dsRNA-containing debris are generated secondary to infection-mediated cell death,[41] and DC phagocytose by-stander dead cells. Likewise, soluble tumor Ags released from tumor cells usually are extrinsically taken up by APC in patients with cancer.[42] If CTL are successfully induced in therapeutic biotherapy targeted against cancer cells, this extrinsic TICAM-1 pathway must be involved in the therapeutic process.

Cross-presentation occurs in a TAP-dependent[43] and -independent fashions.[44,45] The peptides are transported by TAP into the endoplasmic reticulum (ER) and loaded onto MHC Class I for presentation at the cell surface. ER and phagosome might fuse each other for accelerating cross-presentation.[46] Another possibility is that cross-presentation occurs in early endosomes where TLR3 resides. This early endosome cross-presentation does not always depend on TAP[42-44] but requires TLR stimulation.[34] TLR4/MyD88 pathway is involved in the TAP-dependent early endosome model,[43] where recruitment of TAP to the early endosomes is an essential step for the cross-presentation of soluble Ag. These models together with our genechip analysis of polyI:C-stimulated BMDC suggested that some ER-associated proteins are upregulated in BMDC by polyI:C-TICAM-1 pathway. The results infer that the TLR3/TICAM-1 rather than the TLR4/MyD88 pathway more crucially participates in cross-presentation in response to dsRNA or viral stimuli and facilitates raising CTL antitumor immunity in APC.

Although multiple RNA sensors couple with TICAM-1 and signal to activate the Type I IFN-inducing pathway,[25] at least TLR3 in the CD8α+ DC are critical in CTL driving. CD8α+ DC are a high TLR3 expresser, while BMDC express TLR3 with only low levels.[22] CD8α- DC do not express it.[22] The Ag presentation and TLR3 levels in CD8α+ DC appear reciprocally correlated with the phagocytosing ability of DC. Although the TLR3 mRNA level is downregulated secondary to polyI:C response after maturation, this may not be related to the CD8α+ DC functions. Yet, polyI:C might interact with other cytoplasmic sensors for DC maturation,[32,47]

The route of administration and delivery methods may be important for culminate the polyI:C adjuvant function. The toxic problem has not overcome in the adjuvant therapy using polyI:C[35,36] and this is a critical matter for clinical introduction of dsRNA reagents to immunotherapy. The most problematic is the life-threatening shock induced by polyI:C. Recent advance of polyI:C study suggests that PEI-jet helps efficient uptake of polyI:C into peritoneal macrophages.[48] LC (poly-L-lysine and methyl-cellulose) has been used as a preservative to reduce the toxic effect of polyI:C.[49] Nanotechnological delivery of polyI:C results in efficient tumor regression.[50] There are many subsets of DC that can be defined by surface markers, and selecting an appropriate administration route can target a specific DC subset. The route for s.c. administration usually mature dermal/epidermal DC or Langerhans cells.[51,52] Some DC subsets with unique properties specialized to CTL induction would work in association with the route of polyI:C administration. Attempting to develop more harmless and efficient dsRNA derivatives will benefit for establishing human adjuvant immunotherapy for cancer.

Materials and Methods

Mice. TICAM-1$^{-/-}$ and IPS-1$^{-/-}$ mice were made in our laboratory and backcrossed more than eight times to adapt C57BL/6 background.[12] IRF-3/7$^{-/-}$ and IFNAR$^{-/-}$ mice were kindly provided by T. Taniguchi (University of Tokyo, Tokyo, Japan). TLR3$^{-/-}$ mice were kindly provided by S. Akira (Osaka University, Osaka, Japan). Rag2$^{-/-}$ and OT-1 mice were kindly provided from Drs N. Ishii (Tohoku University, Sendai, Japan). Rag2$^{-/-}$/OT-1 mice were bred in our laboratory. All mice were maintained under specific pathogen-free conditions in the animal facility of the Hokkaido University Graduate School of Medicine. Animal experiments were performed according to the guidelines set by the animal safety center, Hokkaido University, Japan.

Cells. EG7 and C1498 cells were purchased from ATCC and cultured in RPMI1640/10% FCS/55 μM 2-ME/1 mM sodium pyruvate and RPMI1640/10% FCS/25 ng/ml 2-ME, respectively. Mouse splenocytes, OT-1 T cell, CD8α+ DC and CD8α- DC were harvested from the spleen and cultured in RPMI1640/10% FCS/55 μM 2-ME/10 mM HEPES.[41] B16D8 cells were cultured in RPMI/10% FCS as described previously.[12]

Reagents and antibodies. Ovalbumin (OVA) and polyI:C (polyI:C) were purchased from SIGMA and Amersham Biosciences, respectively. $OVA_{257-264}$ peptide (SIINFEKL: SL8)

and OVA ($H2K^b$-SL8) Tetramer were from MBL. Following Abs were purchased: anti-CD3ε (145-2C11), anti-CD8β (53-6.7), anti-CD11c (N418), anti-CD16/32 (93), anti-CD69 (H1.2F3) and anti-IFNγ(XMG1.2) Abs from BioLegend, anti-B220 (RA3-6B2), anti-CD4 (L3T4), anti-CD40 (1C10), anti-CD86 (GL1), and anti-MHC I-SL8 (25-D1.16) Abs from eBiosciences, anti-TCR-Vβ5.1/5.2 Ab and ViaProbe from BD Biosciences. The Rat anti-mouse TLR3 mAb (11F8) was kindly provided by David M. Segal (National Institute of Health, Bethesda, MD). To rule out LPS contamination, we treated OVA or other reagents with 200 μg/ml of Polymixin B for 30 min at 37°C before use. Texas Red- or FITC-labeled poly(I:C) was prepared using the 5' EndTag™ Nucleic Acid Labeling System (Vector Laboratories) according to the manufacturers instructions.

Tumor challenge and poly I:C therapy. Mice were shaved at the back and s.c. injected with 200 μl of 2×10^6 syngenic EG7 cells in PBS. Tumor volumes were measured at regular intervals by using a caliper. Tumor volume was calculated by using the formula: Tumor volume (cm^3) = (long diameter) × (short diameter)^2 × 0.4. A volume of 50 μl of a mixture consisting of the lysate of 2×10^5 EG7 cells with or without 50 μg of poly I:C (polyI:C) was s.c. injected around the tumor. We added no other emulsified reagent for immunization since we want to role out the conditional effect of the Ag/polyI:C. The treatments were started when the average of tumor volumes reached at 0.4–0.8 cm^3 and performed twice per week. EG7 lysate were prepared by three times freeze/thaw cycles (-140°C/37°C) in PBS, with removal of cell debris by centrifugation at 6,000 g for 10 min.[53] To deplete CD8 T cells, mice were i.p. injected with hybridoma ascites of anti-CD8β mAb. The dose of antibody and the treatment regimens were determined in preliminary studies by using the same lots of antibody used for the experiments. Depletion of the desired cell populations by this treatment was confirmed by FACS for the entire duration of the study.

Evaluation of T cell activity in tumor-bearing mice. Draining inguinal LN cells were harvested from tumor-bearing mice after 24 h from the last polyI:C treatment. The activity of T cells was evaluated by CD69 expression and IL-2/IFNγ production. These cells were stained with FITC-CD8α, PE-CD69, PerCP/Cy5.5-7AAD and APC-CD3ε. To check cytokine production, LN cells were cultured for 3 d in vitro in the presence or absence of EG7 lysates and IL-2 and IFNγ productions were determined by Cytokine Beads Array (CBA) assay (BD). To assess the cytotoxic activity of CTL, standard ^{51}Cr release assay was performed. For CTL expansion, 2.5×10^6 LN cells were co-cultured with 1.25×10^5 mitomycin C-treated EG7 cells in the presence of 10 U/ml IL-2 for 5 d. Then, LN cells were incubated with ^{51}Cr-labeled EG7 or C1498 cells for 4 h and determined cytotoxic activity. The cell-specific cytotoxicity was calculated with subtracting the cytotoxity for C1498 from for EG7 cells.

Antigen-specific T cell expansion in vivo. Mice were i.p. immunized with 1 mg of OVA and 150 μg of poly I:C. After 7 d, spleens were homogenized and stained with FITC-CD8α and PE-OVA Tetramer for detecting OVA-specific CD8 T cell populations. For intracellular cytokine detection, splenocytes were cultured with or without 100 nM OVA peptide (SIINFEKL; SL8) for 8 h and 10 μg/ml of Brefeldin A (Sigma-Aldrich) was added to the culture in the last 4 h. Then cells were stained with PE-anti-CD8α and fixed/permeabilized with Cytofix/Cytoperm (BD Biosciences) according to manufacturer's instruction. Then, fixed/permeabilized cells were further stained with APC-anti-IFNγ. Stained cells were analyzed with FACSCalibur (BD Biosciences) and FlowJo software (Tree Star).

In vivo CTL assay. The in vivo CTL assay was performed as described.[54] In brief, WT, TICAM-$1^{-/-}$, MAVS$^{-/-}$ and IRF-$3/7^{-/-}$ mice were i.v. administered with PBS, 10 μg of OVA or OVA with 50 μg of polyI:C. After 5 d, 2×10^7 target cells (see below) were i.v. injected to other irrelevant mice and 8 h later, the OVA-specific cytotoxicity was measured by FACSCalibur. Target cells were 1:1 mixture of 2 μM SL8-pulsed, 5 μM CFSE-labeled splenocytes and SL8-unpulesed, 0.5 μM CFSE-labeled splenocytes. OVA-specific cytotoxicity was calculated with a formula: {1-(Primed [$CFSE^{high}$(%)/$CFSE^{low}$(%)]/Unprimed [$CFSE^{high}$(%)/$CFSE^{low}$(%)]} × 100.

DC preparation. DCs were prepared from spleens of mice, as described previously.[55] In brief, collagenase-digested spleen cells were treated with ACK buffer and then washed with PBS twice. Then splenocytes were positively isolated with anti-CD11c MicroBeads. $CD11c^+$ cells were acquired routinely about ≥ 80% purity. Further, to highly purify $CD8\alpha^+$ and $CD8\alpha^-$ DCs, spleen DC were stained with FITC-CD8α, PE-B220, PE/Cy7-CD11c and PerCP5.5-7AAD. $CD8\alpha^+$ or $CD8\alpha^-$ $CD11c^+B220^-$ DCs were purified on FACSAriaII (BD). The purity of the cells was ≥ 98%.

OT-1 proliferation assay. Ten micrograms of OVA with or without 50 μg of polyI:C were i.v. injected to WT, TICAM-$1^{-/-}$, IPS-$1^{-/-}$ and DKO mice. After 4 h, $CD8\alpha^+$ or $CD8\alpha^-$ DC were purified from the spleen. 2.5×10^4 $CD8\alpha^+$ or $CD8\alpha^-$ DC were co-cultured with 5×10^4 1 μM CFSE-labeled $Rag2^{-/-}$/OT-1 T cells for 3 d in 96-well round bottom plate. These cells were stained with PE-anti-TCR-Vβ5.1,5.2 and APC-anti-CD3ε and T cell proliferation was analyzed by CFSE dilution using FACSCalibur. Additionally, IFNγ in the culture supernatant was measured by CBA assay.

Statistical analysis. P-values were calculated with one-way analysis of variance (ANOVA) with Bonferroni's test. Error bars represent the SD or SEM between samples.

Disclosure of Potenial Conflicts of Interest

No potential conflicts of interest were disclosed.

Acknowledgment

We are grateful to Drs. T. Taniguchi (University Tokyo, Tokyo), N. Ishii (Tohoku University, Sendai) and D.M. Segel (NCI, Bethesda) for providing us with IRF-$3/7^{-/-}$ mice, OT-1 mice and anti-monse TLR3 mAb, respectively. Invaluable discussions about the peptide vaccine therapy with Dr. N. Satoh (Sapporo Medical

University, Sapporo) are gratefully acknowledged. We thank Drs H. Takaki, J. Kasamatsu, H.H. Aly, and H. Shime in our lab for their critical comments on this study.

This work was supported in part by Grants-in-Aid from the Ministry of Education, Science, and Culture (Specified Project for Advanced Research, MEXT) and the Ministry of Health, Labor, and Welfare of Japan, and by the Takeda and the Waxmann Foundations. Financial supports by a MEXT Grant-in-Project "The Carcinogenic Spiral" is gratefully acknowledged.

Supplemental Materials

Supplemental materials may be found here:
http://www.landesbioscience.com/journals/oncoimmunology/article/19893/

References

1. Iwasaki A, Medzhitov R. Regulation of adaptive immunity by the innate immune system. Science 2010; 327:291-5; PMID:20075244; http://dx.doi.org/10.1126/science.1183021
2. Seya T, Shime H, Ebihara T, Oshiumi H, Matsumoto M. Pattern recognition receptors of innate immunity and their application to tumor immunotherapy. Cancer Sci 2010; 101:313-20; PMID:20059475; http://dx.doi.org/10.1111/j.1349-7006.2009.01442.x
3. Akira S. Toll-like receptor signaling. J Biol Chem 2003; 278:38105-8; PMID:12893815; http://dx.doi.org/10.1074/jbc.R300028200
4. Kawai T, Akira S. The roles of TLRs, RLRs and NLRs in pathogen recognition. Int Immunol 2009; 21:317-37; PMID:19246554; http://dx.doi.org/10.1093/intimm/dxp017
5. Longman RS, Braun D, Pellegrini S, Rice CM, Darnell RB, Albert ML. Dendritic-cell maturation alters intracellular signaling networks, enabling differential effects of IFN-alpha/beta on antigen cross-presentation. Blood 2007; 109:1113-22; PMID:17018853; http://dx.doi.org/10.1182/blood-2006-05-023465
6. Shinohara ML, Kim JH, Garcia VA, Cantor H. Engagement of the type I interferon receptor on dendritic cells inhibits T helper 17 cell development: role of intracellular osteopontin. Immunity 2008; 29:68-78; PMID:18619869; http://dx.doi.org/10.1016/j.immuni.2008.05.008
7. Diebold SS. Recognition of viral single-stranded RNA by Toll-like receptors. Adv Drug Deliv Rev 2008; 60:813-23; PMID:18241955; http://dx.doi.org/10.1016/j.addr.2007.11.004
8. Matsumoto M, Oshiumi H, Seya T. Antiviral responses induced by the TLR3 pathway. Rev Med Virol 2011. Epub ahead of print. PMID:21312311; http://dx.doi.org/10.1002/rmv.680
9. Yoneyama M, Fujita T. RIG-I family RNA helicases: cytoplasmic sensor for antiviral innate immunity. Cytokine Growth Factor Rev 2007; 18:545-51; PMID:17683970; http://dx.doi.org/10.1016/j.cytogfr.2007.06.023
10. Seya T, Matsumoto M. The extrinsic RNA-sensing pathway for adjuvant immunotherapy of cancer. Cancer Immunol Immunother 2009; 58:1175-84; PMID:19184005; http://dx.doi.org/10.1007/s00262-008-0652-9
11. Akazawa T, Ebihara T, Okuno M, Okuda Y, Shingai M, Tsujimura K, et al. Antitumor NK activation induced by the Toll-like receptor 3-TICAM-1 (TRIF) pathway in myeloid dendritic cells. Proc Natl Acad Sci U S A 2007; 104:252-7; PMID:17190817; http://dx.doi.org/10.1073/pnas.0605978104
12. Ebihara T, Azuma M, Oshiumi H, Kasamatsu J, Iwabuchi K, Matsumoto K, et al. Identification of a polyI:C-inducible membrane protein that participates in dendritic cell-mediated natural killer cell activation. J Exp Med 2010; 207:2675-87; PMID:21059856; http://dx.doi.org/10.1084/jem.20091573
13. Perrot I, Deauvieau F, Massacrier C, Hughes N, Garrone P, Durand I, et al. TLR3 and Rig-like receptor on myeloid dendritic cells and Rig-like receptor on human NK cells are both mandatory for production of IFN-gamma in response to double-stranded RNA. J Immunol 2010; 185:2080-8; PMID:20639488; http://dx.doi.org/10.4049/jimmunol.1000532
14. Bevan MJ. Cross-priming for a secondary cytotoxic response to minor H antigens with H-2 congenic cells which do not cross-react in the cytotoxic assay. J Exp Med 1976; 143:1283-8; PMID:1083422; http://dx.doi.org/10.1084/jem.143.5.1283
15. Datta SK, Redecke V, Prilliman KR, Takabayashi K, Corr M, Tallant T, et al. A subset of Toll-like receptor ligands induces cross-presentation by bone marrow-derived dendritic cells. J Immunol 2003; 170:4102-10; PMID:12682240
16. Schulz O, Diebold SS, Chen M, Näslund TI, Nolte MA, Alexopoulou L, et al. Toll-like receptor 3 promotes cross-priming to virus-infected cells. Nature 2005; 433:887-92; PMID:15711573; http://dx.doi.org/10.1038/nature03326
17. Kono H, Rock KL. How dying cells alert the immune system to danger. Nat Rev Immunol 2008; 8:279-89; PMID:18340345; http://dx.doi.org/10.1038/nri2215
18. Le Bon A, Etchart N, Rossmann C, Ashton M, Hou S, Gewert D, et al. Cross-priming of CD8+ T cells stimulated by virus-induced type I interferon. Nat Immunol 2003; 4:1009-15; PMID:14502286; http://dx.doi.org/10.1038/ni978
19. Bennett SR, Carbone FR, Karamalis F, Miller JF, Heath WR. Induction of a CD8+ cytotoxic T lymphocyte response by cross-priming requires cognate CD4+ T cell help. J Exp Med 1997; 186:65-70; PMID:9206998; http://dx.doi.org/10.1084/jem.186.1.65
20. Shimizu K, Kurosawa Y, Taniguchi M, Steinman RM, Fujii S. Cross-presentation of glycolipid from tumor cells loaded with alpha-galactosylceramide leads to potent and long-lived T cell mediated immunity via dendritic cells. J Exp Med 2007; 204:2641-53; PMID:17923500; http://dx.doi.org/10.1084/jem.20070458
21. Kumar H, Koyama S, Ishii KJ, Kawai T, Akira S. Cutting edge: cooperation of IPS-1- and TRIF-dependent pathways in poly IC-enhanced antibody production and cytotoxic T cell responses. J Immunol 2008; 180:683-7; PMID:18178804
22. Jelinek I, Leonard JN, Price GE, Brown KN, Meyer-Manlapat A, Goldsmith PK, et al. TLR3-specific double-stranded RNA oligonucleotide adjuvants induce dendritic cell cross-presentation, CTL responses, and antiviral protection. J Immunol 2011; 186:2422-9; PMID:21242525; http://dx.doi.org/10.4049/jimmunol.1002845
23. Wang Y, Cella M, Gilfillan S, Colonna M. Cutting edge: polyinosinic:polycytidylic acid boosts the generation of memory CD8 T cells through melanoma differentiation-associated protein 5 expressed in stromal cells. J Immunol 2010; 184:2751-5; PMID:20164430; http://dx.doi.org/10.4049/jimmunol.0903201
24. Carbone FR, Bevan MJ. Induction of ovalbumin-specific cytotoxic T cells by in vivo peptide immunization. J Exp Med 1989; 169:603-12; PMID:2784478; http://dx.doi.org/10.1084/jem.169.3.603
25. Asano J, Tada H, Onai N, Sato T, Horie Y, Fujimoto Y, et al. Nucleotide oligomerization binding domain-like receptor signaling enhances dendritic cell-mediated cross-priming in vivo. J Immunol 2010; 184:736-45; PMID:20008287; http://dx.doi.org/10.4049/jimmunol.0900726
26. McCartney S, Vermi W, Gilfillan S, Cella M, Murphy TL, Schreiber RD, et al. Distinct and complementary functions of MDA5 and TLR3 in poly(I:C)-mediated activation of mouse NK cells. J Exp Med 2009; 206:2967-76; PMID:19995959; http://dx.doi.org/10.1084/jem.20091181
27. Watanabe A, Tatematsu M, Saeki K, Shibata S, Shime H, Yoshimura A, et al. Raftlin is involved in the nucleocapture complex to induce poly(I:C)-mediated TLR3 activation. J Biol Chem 2011; 286:10702-11; PMID:21266579; http://dx.doi.org/10.1074/jbc.M110.185793
28. Itoh K, Watanabe A, Funami K, Seya T, Matsumoto M. The clathrin-mediated endocytic pathway participates in dsRNA-induced IFN-beta production. J Immunol 2008; 181:5522-9; PMID:18832709
29. Talmadge JE, Adams J, Phillips H, Collins M, Lenz B, Schneider M, et al. Immunomodulatory effects in mice of polyinosinic-polycytidylic acid complexed with poly-L-lysine and carboxymethylcellulose. Cancer Res 1985; 45:1058-65; PMID:3155990
30. Conforti R, Ma Y, Morel Y, Paturel C, Terme M, Viaud S, et al. Opposing effects of toll-like receptor (TLR3) signaling in tumors can be therapeutically uncoupled to optimize the anticancer efficacy of TLR3 ligands. Cancer Res 2010; 70:490-500; PMID:20068181; http://dx.doi.org/10.1158/0008-5472.CAN-09-1890
31. Kaiser WJ, Offermann MK. Apoptosis induced by the toll-like receptor adaptor TRIF is dependent on its receptor interacting protein homotypic interaction motif. J Immunol 2005; 174:4942-52; PMID:15814722
32. Zhang Z, Kim T, Bao M, Facchinetti V, Jung SY, Ghaffari AA, et al. DDX1, DDX21, and DHX36 helicases form a complex with the adaptor molecule TRIF to sense dsRNA in dendritic cells. Immunity 2011; 34:866-78; PMID:21703541; http://dx.doi.org/10.1016/j.immuni.2011.03.027
33. Gitlin L, Barchet W, Gilfillan S, Cella M, Beutler B, Flavell RA, et al. Essential role of mda-5 in type I IFN responses to polyriboinosinic:polyribocytidylic acid and encephalomyocarditis picornavirus. Proc Natl Acad Sci U S A 2006; 103:8459-64; PMID:16714379; http://dx.doi.org/10.1073/pnas.0603082103
34. Matsumoto M, Seya T. TLR3: interferon induction by double-stranded RNA including poly(I:C). Adv Drug Deliv Rev 2008; 60:805-12; PMID:18262679; http://dx.doi.org/10.1016/j.addr.2007.11.005

35. Absher M, Stinebring WR. Toxic properties of a synthetic double-stranded RNA. Endotoxin-like properties of poly I. poly C, an interferon stimulator. Nature 1969; 223:715-7; PMID:5805520; http://dx.doi.org/10.1038/223715a0
36. Berry LJ, Smythe DS, Colwell LS, Schoengold RJ, Actor P. Comparison of the effects of a synthetic polyribonucleotide with the effects of endotoxin on selected host responses. Infect Immun 1971; 3:444-8; PMID:16557994
37. Sasai M, Shingai M, Funami K, Yoneyama M, Fujita T, Matsumoto M, et al. NAK-associated protein 1 participates in both the TLR3 and the cytoplasmic pathways in type I IFN induction. J Immunol 2006; 177:8676-83; PMID:17142768
38. Ishikawa H, Barber GN. STING is an endoplasmic reticulum adaptor that facilitates innate immune signalling. Nature 2008; 455:674-8; PMID:18724357; http://dx.doi.org/10.1038/nature07317
39. Taniguchi T, Takaoka A. A weak signal for strong responses: interferon-alpha/beta revisited. Nat Rev Mol Cell Biol 2001; 2:378-86; PMID:11331912; http://dx.doi.org/10.1038/35073080
40. Ogasawara S, Yano H, Momosaki S, Akiba J, Nishida N, Kojiro S, et al. Growth inhibitory effects of IFN-beta on human liver cancer cells in vitro and in vivo. J Interferon Cytokine Res 2007; 27:507-16; PMID: 17572015; http://dx.doi.org/10.1089/jir.2007.0183
41. Ebihara T, Shingai M, Matsumoto M, Wakita T, Seya T. Hepatitis C virus-infected hepatocytes extrinsically modulate dendritic cell maturation to activate T cells and natural killer cells. Hepatology 2008; 48:48-58; PMID:18537195; http://dx.doi.org/10.1002/hep.22337
42. Chaput N, Conforti R, Viaud S, Spatz A, Zitvogel L. The Janus face of dendritic cells in cancer. Oncogene 2008; 27:5920-31; PMID:18836473; http://dx.doi.org/10.1038/onc.2008.270
43. Burgdorf S, Schölz C, Kautz A, Tampé R, Kurts C. Spatial and mechanistic separation of cross-presentation and endogenous antigen presentation. Nat Immunol 2008; 9:558-66; PMID:18376402; http://dx.doi.org/10.1038/ni.1601
44. Shen L, Sigal LJ, Boes M, Rock KL. Important role of cathepsin S in generating peptides for TAP-independent MHC class I crosspresentation in vivo. Immunity 2004; 21:155-65; PMID:15308097; http://dx.doi.org/10.1016/j.immuni.2004.07.004
45. Kurotaki T, Tamura Y, Ueda G, Oura J, Kutomi G, Hirohashi Y, et al. Efficient cross-presentation by heat shock protein 90-peptide complex-loaded dendritic cells via an endosomal pathway. J Immunol 2007; 179:1803-13; PMID:17641047
46. Gagnon E, Duclos S, Rondeau C, Chevet E, Cameron PH, Steele-Mortimer O, et al. Endoplasmic reticulum-mediated phagocytosis is a mechanism of entry into macrophages. Cell 2002; 110:119-31; PMID:12151002; http://dx.doi.org/10.1016/S0092-8674(02)00797-3
47. Samuel CE. Antiviral actions of interferons. Clin Microbiol Rev 2001; 14:778-809; PMID:11585785; http://dx.doi.org/10.1128/CMR.14.4.778-809.2001
48. Wu CY, Yang HY, Monie A, Ma B, Tsai HH, Wu TC, et al. Intraperitoneal administration of poly(I:C) with polyethylenimine leads to significant antitumor immunity against murine ovarian tumors. Cancer Immunol Immunother 2011; 60:1085-96; PMID:21526359; http://dx.doi.org/10.1007/s00262-011-1013-7
49. Longhi MP, Trumpfheller C, Idoyaga J, Caskey M, Matos I, Kluger C, et al. Dendritic cells require a systemic type I interferon response to mature and induce CD4+ Th1 immunity with poly IC as adjuvant. J Exp Med 2009; 206:1589-602; PMID:19564349; http://dx.doi.org/10.1084/jem.20090247
50. Kitano S, Kageyama S, Nagata Y, Miyahara Y, Hiasa A, Naota H, et al. HER2-specific T-cell immune responses in patients vaccinated with truncated HER2 protein complexed with nanogels of cholesteryl pullulan. Clin Cancer Res 2006; 12:7397-405; PMID:17189412; http://dx.doi.org/10.1158/1078-0432.CCR-06-1546
51. Kushwah R, Hu J. Complexity of dendritic cell subsets and their function in the host immune system. Immunology 2011; 133:409-19; PMID:21627652; http://dx.doi.org/10.1111/j.1365-2567.2011.03457.x
52. Asano K, Nabeyama A, Miyake Y, Qiu CH, Kurita A, Tomura M, et al. CD169-positive macrophages dominate antitumor immunity by crosspresenting dead cell-associated antigens. Immunity 2011; 34: 85-95; PMID:21194983; http://dx.doi.org/10.1016/j.immuni.2010.12.011
53. Galea-Lauri J, Wells JW, Darling D, Harrison P, Farzaneh F. Strategies for antigen choice and priming of dendritic cells influence the polarization and efficacy of antitumor T-cell responses in dendritic cell-based cancer vaccination. Cancer Immunol Immunother 2004; 53:963-77; PMID:15146294; http://dx.doi.org/10.1007/s00262-004-0542-8
54. Durand V, Wong SY, Tough DF, Le Bon A. Shaping of adaptive immune responses to soluble proteins by TLR agonists: a role for IFN-α/β. Immunol Cell Biol 2004; 82:596-602; PMID:15550117; http://dx.doi.org/10.1111/j.0818-9641.2004.01285.x
55. Yamazaki S, Okada K, Maruyama A, Matsumoto M, Yagita H, Seya T. TLR2-dependent induction of IL-10 and Foxp3+ CD25+ CD4+ regulatory T cells prevents effective anti-tumor immunity induced by Pam2 lipopeptides in vivo. PLoS One 2011; 6:e18833; PMID:21533081; http://dx.doi.org/10.1371/journal.pone.0018833

Toll-like receptor 3 signaling converts tumor-supporting myeloid cells to tumoricidal effectors

Hiroaki Shime[a], Misako Matsumoto[a], Hiroyuki Oshiumi[a], Shinya Tanaka[b], Akio Nakane[c], Yoichiro Iwakura[d], Hideaki Tahara[e], Norimitsu Inoue[f], and Tsukasa Seya[a,1]

[a]Department of Microbiology and Immunology, and [b]Department of Cancer Pathology, Graduate School of Medicine, Hokkaido University, Kita-ku, Sapporo 060-8638, Japan; [c]Department of Microbiology and Immunology, Graduate School of Medicine, Hirosaki University, Zaifu-cho, Hirosaki 036-8562, Japan; [d]Laboratory of Molecular Pathogenesis, Center for Experimental Medicine and Systems Biology, and [e]Department of Surgery and Bioengineering, Advanced Clinical Research Center, Institute of Medical Science, University of Tokyo, Shirokanedai, Minato-ku, Tokyo 108-8639, Japan; and [f]Department of Molecular Genetics, Osaka Medical Center for Cancer, Nakamichi, Higashinari-ku, Osaka 537-8511, Japan

Edited by Ruslan Medzhitov, Yale University School of Medicine, New Haven, CT, and approved December 20, 2011 (received for review August 11, 2011)

Smoldering inflammation often increases the risk of progression for malignant tumors and simultaneously matures myeloid dendritic cells (mDCs) for cell-mediated immunity. PolyI:C, a dsRNA analog, is reported to induce inflammation and potent antitumor immune responses via the Toll-like receptor 3/Toll–IL-1 receptor domain-containing adaptor molecule 1 (TICAM-1) and melanoma differentiation-associated protein 5/IFN-β promoter stimulator 1 (IPS-1) pathways in mDCs to drive activation of natural killer cells and cytotoxic T lymphocytes. Here, we found that i.p. or s.c. injection of polyI:C to Lewis lung carcinoma tumor-implant mice resulted in tumor regression by converting tumor-supporting macrophages (Mfs) to tumor suppressors. F4/80^{+}/Gr1^{-} Mfs infiltrating the tumor respond to polyI:C to rapidly produce inflammatory cytokines and thereafter accelerate M1 polarization. TNF-α was increased within 1 h in both tumor and serum upon polyI:C injection into tumor-bearing mice, followed by tumor hemorrhagic necrosis and growth suppression. These tumor responses were abolished in TNF-α$^{-/-}$ mice. Furthermore, F4/80^{+} Mfs in tumors extracted from polyI:C-injected mice sustained Lewis lung carcinoma cytotoxic activity, and this activity was partly abrogated by anti–TNF-α Ab. Genes for supporting M1 polarization were subsequently up-regulated in the tumor-infiltrating Mfs. These responses were completely abrogated in TICAM-1$^{-/-}$ mice, and unaffected in myeloid differentiation factor 88$^{-/-}$ and IPS-1$^{-/-}$ mice. Thus, the TICAM-1 pathway is not only important to mature mDCs for cross-priming and natural killer cell activation in the induction of tumor immunity, but also critically engaged in tumor suppression by converting tumor-supporting Mfs to those with tumoricidal properties.

Toll-like receptor | tumor-associated macrophages | TRIF

Inflammation followed by bacterial and viral infections triggers a high risk of cancer and promotes tumor development and progression (1, 2). Long-term use of anti-inflammatory drugs has been shown to reduce—if not eliminate—the risk of cancer, as demonstrated by a clinical study of aspirin and colorectal cancer occurrence (3). Inflammatory cytokines facilitate tumor progression and metastasis in most cases. Innate immune response and the following cellular events are closely concerned with the formation of the tumor microenvironment (4, 5).

By contrast, inflammation induced by microbial preparations was applied to patients with cancer for therapeutic potential as Coley vaccine with some success. A viral replication product, dsRNA and its analog polyI:C (6, 7), induced acute inflammation, and has been expected to be a promising therapeutic agent against cancer. Although polyI:C exerts life-threatening cytokinemia (8), trials for its clinical use as an adjuvant continued because of its high therapeutic potential (9, 10). Pathogen-associated molecular patterns (PAMPs) and host cell factors induced secondary to PAMP–host cell interaction act as a double-edged sword in cancer prognosis and require understanding their multifarious functional properties in the tumor environment.

Recent advances in the study of innate immunity show how polyI:C suppresses tumor progression (11). PolyI:C is a synthetic compound that serves as an agonist for pattern-recognition receptors (PRRs), Toll-like receptor 3 (TLR3), and melanoma differentiation-associated protein 5 (MDA5) (12–14). Although TLR3 and MDA5 signals are characterized as myeloid differentiation factor 88 (MyD88) independent (15, 16), they have immune effector-inducing properties (12–14, 17). TLR3 couples with the Toll–IL-1 receptor domain-containing adaptor molecule 1 (TICAM-1, also known as TRIF), and MDA5 couples with the IFN-β promoter stimulator 1 (IPS-1, also known as Cardif, MAVS, or VISA) (11, 15). Possible functions for the TICAM-1 and IPS-1 signaling pathways have been investigated by using gene-disrupted mice (15); although they activate the same downstream transcription factors NF-κB and IFN regulatory factor 3 (IRF-3) (15, 18), they appear to distinctly modulate myeloid dendritic cells (mDCs) and macrophages (Mfs) to drive effector lymphocytes (19, 20).

Tumor microenvironments frequently involve myeloid-derived suppressor cells (MDSCs), tumor-associated macrophages (TAMs), and immature mDCs (1, 21). These myeloid cells express PRR through which they are functionally activated. Once the inflammation process is triggered, immature mDCs turn mature so that they are capable of antigen cross-presentation and able to activate immune effector cells, which would act to protect the host system and damage the undesirable tumor cells (22). However, TAMs and MDSCs play a major role in establishing a favorable environment for tumor cell development by suppressing antitumor immunity and recruiting host immune cells to support tumor cell survival, motility, and invasion (23–25). Although these myeloid cell scenarios have been studied with interest, how the PRR signal in these myeloid cells links regulation of tumor progression has yet to be elucidated.

Here we show that TICAM-1 but not IPS-1 signal in tumor-infiltrating Mfs is engaged in conversion of the TAM-like Mfs to tumoricidal effectors. We investigated the molecular mechanisms in Mfs underlying the phenotype switch from tumor supporting to tumor suppressing by treating cells with polyI:C and found that the TICAM-1–inducing TNF-α and M1 polarization are crucial for eliciting tumoricidal activity in TAMs.

Results

In Vivo Effect of PolyI:C on Implant Lewis Lung Carcinoma Tumor. I.p. injection of polyI:C rapidly induced hemorrhagic necrosis in 3LL tumors implanted in WT mice, which was established >12 h after polyI:C treatment (Fig. 1*A*). The polyI:C-dependent hemorrhagic necrosis did not occur in TNF-α$^{-/-}$ mice (Fig. 1*A*). Histological

Author contributions: H.S., M.M., and T.S. designed research; H.S., H.O., and S.T. performed research; H.O., A.N., Y.I., and H.T. contributed new reagents/analytic tools; M.M. and N.I. analyzed data; and H.S. and T.S. wrote the paper.

The authors declare no conflict of interest.

This article is a PNAS Direct Submission.

[1]To whom correspondence should be addressed. E-mail: seya-tu@pop.med.hokudai.ac.jp.

This article contains supporting information online at www.pnas.org/lookup/suppl/doi:10.1073/pnas.1113099109/-/DCSupplemental.